

Suppressor of Cytokine Signaling-1 Peptidomimetic Limits Progression of Diabetic Nephropathy

Carlota Recio,^{*†‡} Iolanda Lazaro,^{*†} Ainhoa Oguiza,^{*†‡} Laura Lopez-Sanz,^{*†} Susana Bernal,^{*†} Julia Blanco,[§] Jesus Egido,^{†‡} and Carmen Gomez-Guerrero^{*†‡}

^{*}Renal and Vascular Inflammation Group and [†]Division of Nephrology and Hypertension, Fundacion Jimenez Diaz University Hospital-Health Research Institute, Autonoma University of Madrid; [‡]Spanish Biomedical Research Centre in Diabetes and Associated Metabolic Disorders; and [§]Department of Pathology, Hospital Clinico San Carlos, Madrid, Spain

ABSTRACT

Diabetes is the main cause of CKD and ESRD worldwide. Chronic activation of Janus kinase and signal transducer and activator of transcription (STAT) signaling contributes to diabetic nephropathy by inducing genes involved in leukocyte infiltration, cell proliferation, and extracellular matrix accumulation. This study examined whether a cell-permeable peptide mimicking the kinase-inhibitory region of suppressor of cytokine signaling-1 (SOCS1) regulatory protein protects against nephropathy by suppressing STAT-mediated cell responses to diabetic conditions. In a mouse model combining hyperglycemia and hypercholesterolemia (streptozotocin diabetic, apoE-deficient mice), renal STAT activation status correlated with the severity of nephropathy. Notably, compared with administration of vehicle or mutant inactive peptide, administration of the SOCS1 peptidomimetic at either early or advanced stages of diabetes ameliorated STAT activity and resulted in reduced serum creatinine level, albuminuria, and renal histologic changes (mesangial expansion, tubular injury, and fibrosis) over time. Mice treated with the SOCS1 peptidomimetic also exhibited reduced kidney leukocyte recruitment (T lymphocytes and classic M1 proinflammatory macrophages) and decreased expression levels of proinflammatory and profibrotic markers that were independent of glycemic and lipid changes. *In vitro*, internalized peptide suppressed STAT activation and target gene expression induced by inflammatory and hyperglycemic conditions, reduced migration and proliferation in mesangial and tubulointerstitial cells, and altered the expression of cytokine-induced macrophage polarization markers. In conclusion, our study identifies SOCS1 mimicking as a feasible therapeutic strategy to halt the onset and progression of renal inflammation and fibrosis in diabetic kidney disease.

J Am Soc Nephrol 28: 575–585, 2017. doi: 10.1681/ASN.2016020237

Diabetic nephropathy (DN) is a relevant, chronic, microvascular complication in terms of morbidity and mortality for patients with diabetes mellitus in Western countries.¹ The progression of DN is characterized by an increase in urinary albumin excretion, hypertension, glomerulosclerosis, and an eventual reduction in GFR, leading to ESRD. These functional changes are related to a remodeling of the renal structure, including glomerular and tubular hypertrophy, inflammation, and extracellular matrix accumulation.² Although hyperglycemia is the driving force for diabetic complications, mounting evidence suggests that dyslipidemia and chronic inflammation are contributory factors

to the progression of diabetic kidney disease. In fact, high-glucose conditions lead to activation of inflammatory mediators in glomerular and tubular cells, which triggers leukocyte infiltration, renal

Received February 29, 2016. Accepted July 4, 2016.

I.L. and A.O. contributed equally to this work.

Correspondence: Dr. Carmen Gomez-Guerrero, Renal and Vascular Inflammation, Fundacion Jimenez Diaz University Hospital-Health Research Institute, Autonoma University of Madrid, Avda. Reyes Catolicos, 2 28040, Madrid, Spain. Email: cgomez@fjd.es; c.gomez@uam.es

Copyright © 2017 by the American Society of Nephrology

cell proliferation, and extracellular matrix expansion.³ Current treatments for diabetic complications based on the integrated control of glycemia, BP, and lipids are insufficient to prevent the progression of CKD in a large proportion of patients^{1,4,5}; as such, there is a clear need for new strategies to slow the decline of renal function in DN.

The Janus kinase (JAK)/signal transducers and activators of transcription (STAT) signaling pathway regulates a broad range of mediators implicated in cell proliferation, differentiation, recruitment, and fibrosis and is an important mechanism through which hyperglycemia and inflammation contribute to chronic and acute kidney diseases.^{6–8} Four kinases (JAK1–3 and TYK2) and seven transcription factors (STAT1–4, 5A, 5B, and 6) constitute the family, and cell-specific JAK/STAT combinations have been paired with each receptor type.⁹ Upon ligand binding, activated JAK phosphorylates the receptor cytoplasmic domain to allow recruitment and tyrosine phosphorylation of latent STATs, causing them to form homo- or heterodimers and translocate to the nucleus, where they activate gene expression.¹⁰

SOCS proteins are key negative regulators that control the magnitude and duration of JAK/STAT signaling through several mechanisms, including kinase inhibition, STAT binding, and targeting for proteasomal degradation.^{11–13} SOCS family members (CIS and SOCS1–7) contain a variable N-terminal domain, a central SH2 domain, and a conserved C-terminal SOCS box involved in proteasomal targeting. The most relevant members (SOCS1 and SOCS3) also contain a 12-amino acid N-terminal kinase inhibitory region (KIR) essential for inhibition of JAK tyrosine kinase activity.^{11,13}

Dysregulated JAK/STAT contributes to the pathogenesis of autoimmune diseases, inflammation, and cancer,¹² and also plays an important role in the onset and progression of diabetes and its chronic vascular complications (e.g., nephropathy, retinopathy, neuropathy, and atherosclerosis).^{5,8,14} Different strategies based on the regulatory role of the SOCS family have been proposed as potential anti-inflammatory therapy for these conditions.¹³ Accordingly, the present work investigates the

renoprotective properties of a cell-permeable peptide mimicking the activity of the SOCS1 KIR region to impair pathologic JAK/STAT activity in a mouse model of DN and in cultured renal cells under diabetic conditions.

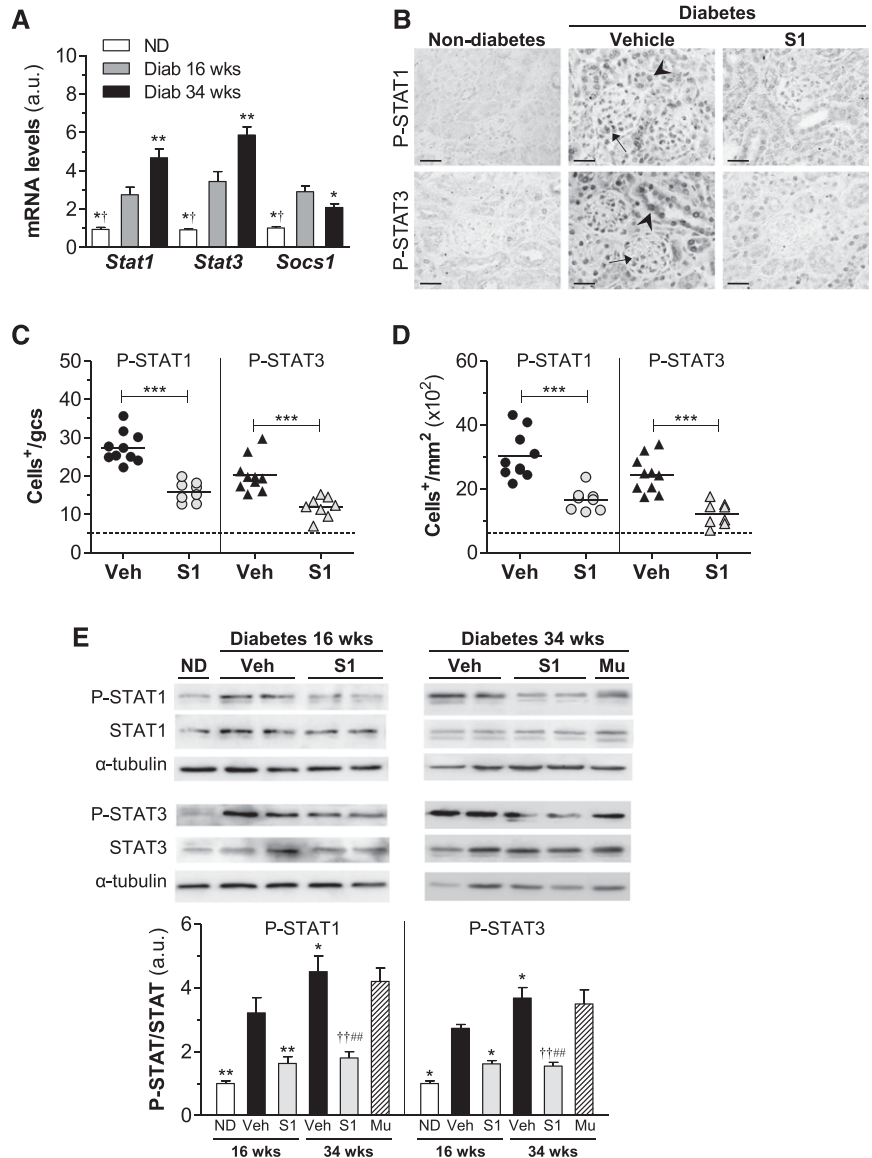


Figure 1. SOCS1 peptide inhibits STAT activation in diabetic kidneys. (A) *Stat1*, *Stat3*, and *Socs1* gene expression in renal cortex from nondiabetic and diabetic mice in early (aged 16 weeks) and late (aged 34 weeks) disease checkpoints was analyzed using real-time PCR, normalized by 18S endogenous control and expressed in arbitrary units (a.u.). (B–D) Immunostaining of P-STAT1 and P-STAT3 in kidney sections from nondiabetic and diabetic mice (early model). Representative micrographs (B) and quantification of positive cells in glomeruli (C) and tubulointerstitium (D) are shown. Horizontal dotted lines represent the mean values for nondiabetic mice. (E) Western blot of P-STAT1 and P-STAT3 in renal cortical lysates in the early and late models of diabetes. Shown are representative images and the summary of normalized quantification, expressed in a.u. Diab, diabetic; ND, nondiabetic; Veh, vehicle. * $P < 0.05$, ** $P < 0.01$, and *** $P < 0.001$ versus Veh (16 weeks); † $P < 0.05$ and †† $P < 0.01$ versus Veh (34 weeks), # $P < 0.05$ and ## $P < 0.01$ versus Mu. Original magnification, $\times 200$ in B.

RESULTS

SOCS1 Peptide Inhibits JAK/STAT Activation in Diabetic Kidneys

The therapeutic potential of SOCS1 peptidomimetic was investigated in streptozotocin-induced diabetic and apoE-deficient mice, an experimental model of DN that combines hyperglycemia and hypercholesterolemia, two important risk factors of this disease.¹⁵ Biodistribution and pharmacokinetic studies of rhodamine-labeled SOCS1 peptide (administered *via* the intraperitoneal route) revealed efficient accumulation in kidney (glomerular and tubular localization), spleen, and liver of mice (Supplemental Figure 1, A and B). Maximal fluorescence in plasma and urine were reached at 4 and 6 hours, respectively (Supplemental Figure 1C), with a plasma elimination $t_{1/2}$ of 4.5 hours (Supplemental Figure 1D).

Diabetic mice were treated with SOCS1 peptide (S1 group), mutant inactive peptide (Mu group), and vehicle at either an early (10–16 weeks of age) or later (24–34 weeks of age) disease stage. We first analyzed the time course of STAT1, STAT3, and SOCS1 mRNA expression during the progression of DN. In contrast to the gradual rise in STATs over time, SOCS1 expression showed an initial increase followed by a significant decrease at later stage of DN (Figure 1A). Furthermore, immunohistochemistry to detect the activation status of STAT proteins in the kidney revealed an intense nuclear staining of phosphorylated STAT1 (P-STAT1) and P-STAT3 in glomeruli and tubulointerstitium of diabetic mice receiving vehicle, a significant reduction (approximately 50%) in SOCS1-treated mice (Figure 1, B–D), and also a positive correlation between the two variables in the experimental groups (Supplemental Figure 2). Western blot analysis (Figure 1E) further confirmed attenuated P-STAT1/3 levels by SOCS1 peptide both at early

and late treatment stages, whereas the mutant sequence (Mu group) was ineffective.

SOCS1 Peptide Ameliorates Diabetic Kidney Disease

Diabetes was associated with a progressive renal decline, as demonstrated by an increased urine albumin-to-creatinine ratio (UAC; Supplemental Figure 3, B and C) and serum creatinine (Table 1). These parameters were significantly improved in S1 groups compared with respective vehicle groups both at early and late treatment stages, with percentages of decrease ranging from 33% to 42% (Figure 2A, Table 1). SOCS1 peptide also ameliorated kidney/body weight ratio (Table 1) and the renal expression of kidney injury molecule-1 (Figure 2B). By contrast, no significant differences were observed between the vehicle and Mu groups, thus excluding any off-target effects. Neither early nor late treatments affected hyperglycemia (blood glucose and glycated hemoglobin), lipid profile, or body weight in diabetic mice (Supplemental Figure 3, D–G, Table 1). Furthermore, no signs of toxicity or hepatic or splenic damage were observed in the treated groups (not shown).

Histologic assessment of periodic acid–Schiff (PAS)–stained kidney samples revealed that SOCS1 peptide attenuated several morphologic changes within the glomerulus (hypercellularity, mesangial matrix expansion, and capillary dilation), tubules (atrophy and degeneration), and interstitium (fibrosis and inflammatory infiltrate) of diabetic mice (Figure 2C, Table 2). Digital quantification further confirmed that SOCS1 intervention decreased glomerular size (percent reduction versus vehicle: 16 weeks, 41 ± 2 ; 34 weeks, 36 ± 3 ; Figure 2D) and PAS⁺-mesangial area (percent reduction: 16 weeks, 51 ± 4 ; 34 weeks, 33 ± 6 ; Figure 2E). Furthermore, Pearson test showed significant correlations between P-STAT1/P-STAT3 levels and indicators of renal damage (Table 3).

Table 1. General and metabolic variables of nondiabetic and diabetic mice at the end of the experimental models

| Variables | Early Model (Age, 16 wk) | | | Late Model (Age, 34 wk) | | |
|-------------------------|--------------------------|------------|------------------------|-------------------------|--------------------------|------------|
| | Nondiabetes (n=5) | Diabetes | | Diabetes | | |
| | | Veh (n=10) | S1 (n=8) | Veh (n=8) | S1 (n=6) | Mu (n=5) |
| ΔBody wt, g | 3.2±0.2 ^a | −(2.3±0.5) | −(2.0±0.3) | −(2.8±0.6) | −(2.3±0.5) | −(2.6±0.2) |
| KBWR, g/kg | 14.0±0.4 ^a | 17.9±0.4 | 16.1±0.3 ^b | 19.0±0.3 | 16.3±0.8 ^{d,e} | 18.4±0.3 |
| SCr, mmol/L | 0.28±0.08 ^a | 1.11±0.06 | 0.68±0.06 ^c | 1.30±0.12 | 0.73±0.07 ^{d,e} | 1.20±0.14 |
| BG, mmol/L | 7.7±0.6 ^a | 27.8±1.3 | 28.2±0.6 | 27.5±1.0 | 27.3±1.0 | 28.1±1.4 |
| HbA1c, μg/ml | 120±2 ^a | 490±37 | 504±45 | 522±5 | 510±14 | 515±18 |
| Chol, mmol/L | 8.0±0.2 ^a | 14.0±0.3 | 14.7±0.6 | 22.7±1.9 | 21.9±1.8 | 22.9±1.6 |
| LDL-cholesterol, mmol/L | 7.8±0.5 ^a | 14.4±0.4 | 15.1±0.5 | 20.8±2.7 | 19.7±2.5 | 21.0±0.6 |
| HDL-cholesterol, mmol/L | 0.32±0.02 | 0.28±0.05 | 0.26±0.02 | 0.51±0.05 | 0.55±0.06 | 0.53±0.03 |
| TG, mmol/L | 0.55±0.06 | 0.89±0.05 | 0.93±0.14 | 1.32±0.20 | 1.36±0.21 | 1.31±0.06 |

Results from the different groups of nondiabetic and diabetic are reported as mean ± SEM and analyzed by two-way ANOVA followed by Bonferroni *post hoc* test.

Veh, vehicle; ΔBody wt, body weight change (final – initial); KBWR, kidney/body weight ratio; SCr, serum creatinine; BG, blood glucose; HbA1c, glycated hemoglobin; Chol, cholesterol; TG, triglyceride.

^aP<0.001.

^bP<0.01.

^cP<0.05 versus Veh (16 weeks).

^dP<0.01 versus Veh (34 weeks).

^eP<0.05 versus Mu.

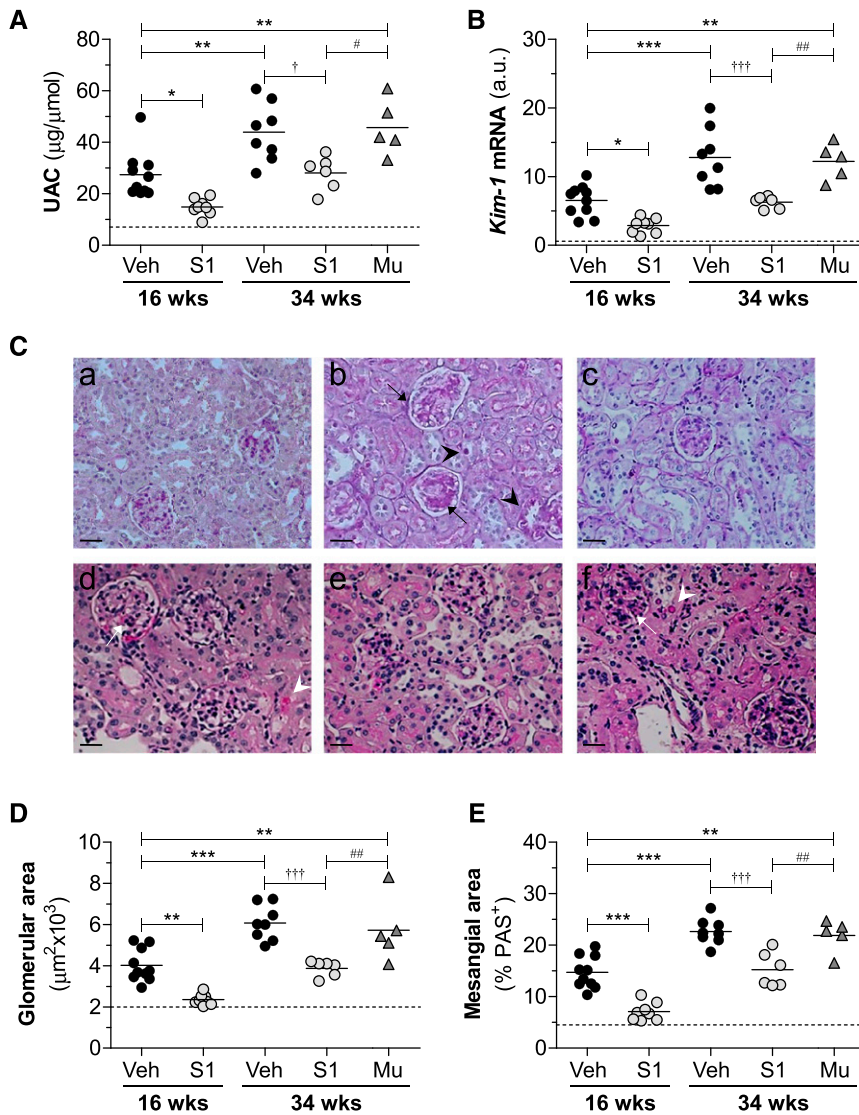


Figure 2. SOCS1 peptide protects from diabetes-associated renal injury in apoE-deficient mice. (A) Albuminuria levels in apoE-deficient mice at early (age 16 weeks) and late (age 34 weeks) diabetes. (B) Gene expression of kidney injury molecule (*Kim-1*) in renal cortex was analyzed by real-time PCR, normalized by 18S endogenous control, and expressed in arbitrary units (a.u.). (C) Representative images of PAS-stained kidney sections from mice in the early (age 16 weeks; a–c) and late (age 34 weeks; d–f) diabetes models: nondiabetes (a), diabetes+vehicle (b and d), diabetes+S1 (c and e), and diabetes+Mu (f). Diabetic mice exhibited glomerular hypertrophy/PAS⁺ area expansion (arrows) and tubular atrophy/glycogen deposition (arrowheads). Milder damage was observed in S1 groups. (D) Glomerular area quantification in the experimental groups. (E) PAS⁺ mesangial area analysis. Veh, vehicle. **P*<0.05, ***P*<0.01, and ****P*<0.001 versus Veh (16 weeks); †*P*<0.05 and †††*P*<0.001 versus Veh (34 weeks); #*P*<0.05 and ##*P*<0.01 versus Mu. Horizontal dotted lines represent the mean values for nondiabetic mice in A, B, D, and E. Original magnification, ×200 in C.

Antifibrotic and Anti-Inflammatory Effects of SOCS1 Peptide

Overproduction of extracellular matrix is a hallmark of DN and leads to glomerular sclerosis and interstitial fibrosis.^{5,16} Analysis of picrosirius red staining (Figure 3A) in diabetic kidneys

revealed a progressive accumulation of collagen in glomeruli and tubulointerstitium. Furthermore, S1 groups of diabetic mice exhibited a 44%–38% reduction (*P*<0.01) of renal fibrosis over time compared with age-matched vehicle mice, whereas mutant peptide had no antifibrotic effect (Figure 3, A–C). Accordingly, SOCS1 peptide attenuated the mRNA (Figure 3D) and protein (Figure 3E) expression levels of fibrotic markers (type I collagen, fibronectin, and TGFβ), which positively correlated with P-STAT1/3 activation (Table 3).

The induction of diabetes was associated with the recruitment, retention, and activation of leukocytes in mouse kidney, as evidenced by increased expression of leukocyte markers and proinflammatory genes (Figure 4). SOCS1-treated mice exhibited a significant reduction (approximately 50%) in the number of infiltrating CD3⁺ T lymphocytes and F4/80⁺ macrophages (Figure 4, A–C), in good correlation with STAT activation levels (Table 3). Furthermore, peptide treatment decreased the gene and/or protein expression levels of monocyte and T cell chemokines (CC chemokine ligand [CCL] 2 and CCL5) and cytokine TNFα in diabetic kidneys (Figure 4, D and E).

To further evaluate whether SOCS1 peptide modulates the functional stage of kidney macrophages, expression levels of arginase isoforms (ArgII and ArgI) were analyzed to distinguish between proinflammatory M1 and anti-inflammatory M2 phenotypes, respectively. Both macrophage phenotypes are present in diabetic kidneys, ArgII (M1) being the most abundantly expressed in the vehicle group and ArgI (M2) the predominant macrophage marker in the S1 group (Figure 4, F and G). Consistently, SOCS1-treated mice displayed a decreased Ly6C^{high}/Ly6C^{low} ratio of circulating monocytes (Figure 4H).

In Vitro Effects of SOCS1 Peptide

To corroborate the experimental model we assessed, *in vitro*, the effect of SOCS1 peptide on murine mesangial cells (MC), tubuloepithelial cells (MCT), and macrophages stimulated with either inflammatory cytokines (IFNγ-plus IL-6) or high-glucose concentrations (HG) in an attempt to mimic the diabetic milieu. Efficient cytoplasmic uptake of rhodamine-labeled peptide was visualized *via* confocal microscopy (Supplemental Figure 4). Internalized SOCS1

Table 2. Renal scores of nondiabetic and diabetic mice at 16 weeks of age

| Histological Lesions | Nondiabetes (n=5) | Diabetes | |
|----------------------------|------------------------|------------|------------------------|
| | | Veh (n=10) | S1 (n=8) |
| Glomerular lesions | | | |
| Hypercellularity | 0.20±0.19 ^a | 2.00±0.23 | 0.21±0.15 ^a |
| Mesangial matrix expansion | 0.20±0.20 ^a | 2.30±0.21 | 0.38±0.18 ^a |
| Capillary dilation | 0.00±0.00 ^a | 1.70±0.30 | 0.63±0.18 ^c |
| Tubular lesions | | | |
| Degeneration | 0.40±0.24 ^a | 2.00±0.26 | 0.50±0.19 ^a |
| Atrophy | 0.20±0.20 ^a | 1.90±0.28 | 0.63±0.26 ^b |
| Interstitial lesions | | | |
| Fibrosis | 0.00±0.00 ^b | 1.20±0.33 | 0.25±0.16 ^c |
| Inflammation | 0.10±0.14 ^a | 1.80±0.23 | 0.38±0.20 ^a |

PAS-stained renal samples were semiquantitatively graded (0–3 scale) in a blinded manner according to the extent of glomerular, tubular, and interstitial damage. Results from the different groups of mice are reported as means±SEM and analyzed by two-way ANOVA followed by Bonferroni *post hoc* test. Veh, vehicle.

^aP<0.001.

^bP<0.01.

^cP<0.05 versus Veh.

peptide, but not the Mu sequence, further inhibited phosphorylation (Figure 5, A and B) and nuclear translocation (Supplemental Figure 4) of STAT1/3, and also prevented proinflammatory and profibrotic gene expression (Figure 5, C and D, Supplemental Figure 5A) in renal cells exposed to diabetic stimulation. Likewise, SOCS1 peptide attenuated the secretion of CCL2, CCL5 (Figure 5E, Supplemental Figure 5B), and fibronectin (Figure 5F) induced by cytokines in renal cells. In these experiments, the inhibitory effect of SOCS1 peptide was very similar to that observed after the silencing

of STAT1 with specific small interfering RNA, used as positive control (Supplemental Figure 6).

To evaluate the functional consequences of inflammatory gene reduction, we next examined the effect of SOCS1 peptide on cell migration, proliferation, and differentiation—important processes involved in renal damage during DN. *In vitro* wound-healing assay with MC demonstrated the antimigratory effect of SOCS1, but not mutant peptide (Figure 6A). SOCS1 peptide was also able to prevent the mitogenic effect of cytokines (Figure 6, B and C) and high-glucose levels (Figure 6D) on renal cells, without affecting cell viability. Furthermore, in cytokine-induced macrophages, SOCS1 peptide inhibited M1 in favor of M2 phenotype, as evidenced by significantly downregulated ArgII and increased expression of ArgI (Figure 6E, Supplemental Figure 5C).

DISCUSSION

Delaying the progression of nephropathy toward end-stage renal failure remains a primary goal in the treatment of diabetes. Beyond current therapies with limited improvement of renal function,^{1,4,5} novel approaches involving the inhibition of pathologic factors and the promotion of protective/reparative mechanisms are of clinical interest. Herein, we report that a peptide mimicking the endogenous regulatory protein SOCS1 counteracts DN with overactive JAK/STAT signaling by reducing renal inflammation and fibrosis, manifested by an improvement in albuminuria and renal function.

The JAK2/STAT1/3-dependent axis is preferentially active in diabetes^{6,8} and mediates the effects of diabetic factors in renal cells by inducing the transcription of inflammatory

Table 3. Correlation of STAT activation levels and renal function in diabetic mice.

| Variables | Glomeruli | | Tubulointerstitium | |
|----------------------------------|----------------------------|----------------------------|----------------------------|----------------------------|
| | P-STAT1 ⁺ Cells | P-STAT3 ⁺ Cells | P-STAT1 ⁺ Cells | P-STAT3 ⁺ Cells |
| | Pearson <i>r</i> (P Value) |
| KBWR, g/kg | 0.6055 (<0.01) | 0.7109 (<0.001) | 0.4717 (<0.05) | 0.5995 (<0.01) |
| UAC, μg/μmol | 0.5991 (<0.01) | 0.7149 (<0.001) | 0.7423 (<0.001) | 0.6723 (<0.01) |
| SCr, mmol/L | 0.7719 (<0.01) | 0.6587 (<0.01) | 0.6646 (<0.01) | 0.5635 (<0.05) |
| Glomerular area, μm ² | 0.9058 (<0.001) | 0.8097 (<0.001) | N.D. | N.D. |
| Mesangial area, % PAS | 0.6822 (<0.01) | 0.4587 (NS) | N.D. | N.D. |
| Fibrosis, % sirius red | 0.6608 (<0.01) | 0.6963 (<0.01) | 0.6185 (<0.01) | 0.7312 (<0.001) |
| T cells, CD3 ⁺ | 0.7011 (<0.01) | 0.7621 (<0.001) | 0.6417 (<0.01) | 0.6082 (<0.01) |
| Macrophages, F4/80 ⁺ | 0.6793 (<0.01) | 0.7954 (<0.001) | 0.6847 (<0.01) | 0.5603 (<0.02) |
| <i>Kim-1</i> mRNA, a.u. | 0.6886 (<0.01) | 0.4226 (NS) | 0.5866 (<0.01) | 0.5592 (<0.02) |
| <i>Ccl2</i> mRNA, a.u. | 0.8077 (<0.001) | 0.7229 (<0.001) | 0.7942 (<0.001) | 0.8257 (<0.001) |
| <i>Ccl5</i> mRNA, a.u. | 0.7662 (<0.001) | 0.6541 (<0.01) | 0.6608 (<0.01) | 0.5621 (<0.02) |
| <i>Tnfa</i> mRNA, a.u. | 0.6726 (<0.01) | 0.7607 (<0.001) | 0.6502 (<0.01) | 0.6262 (<0.01) |
| <i>Col 1</i> mRNA, a.u. | 0.7594 (<0.001) | 0.6959 (<0.01) | 0.7824 (<0.001) | 0.8384 (<0.001) |
| <i>Fn</i> mRNA, a.u. | 0.8198 (<0.001) | 0.7768 (<0.001) | 0.8386 (<0.001) | 0.7230 (<0.001) |
| <i>Tgfb</i> mRNA, a.u. | 0.7893 (<0.001) | 0.6412 (<0.01) | 0.6869 (<0.01) | 0.6777 (<0.01) |

Pearson correlation analysis between P-STAT1/3 immunostaining and renal variables in diabetic mice at 16 weeks of age. KBWR, kidney/body weight ratio; SCr, serum creatinine; N.D., not determined; a.u., arbitrary units.

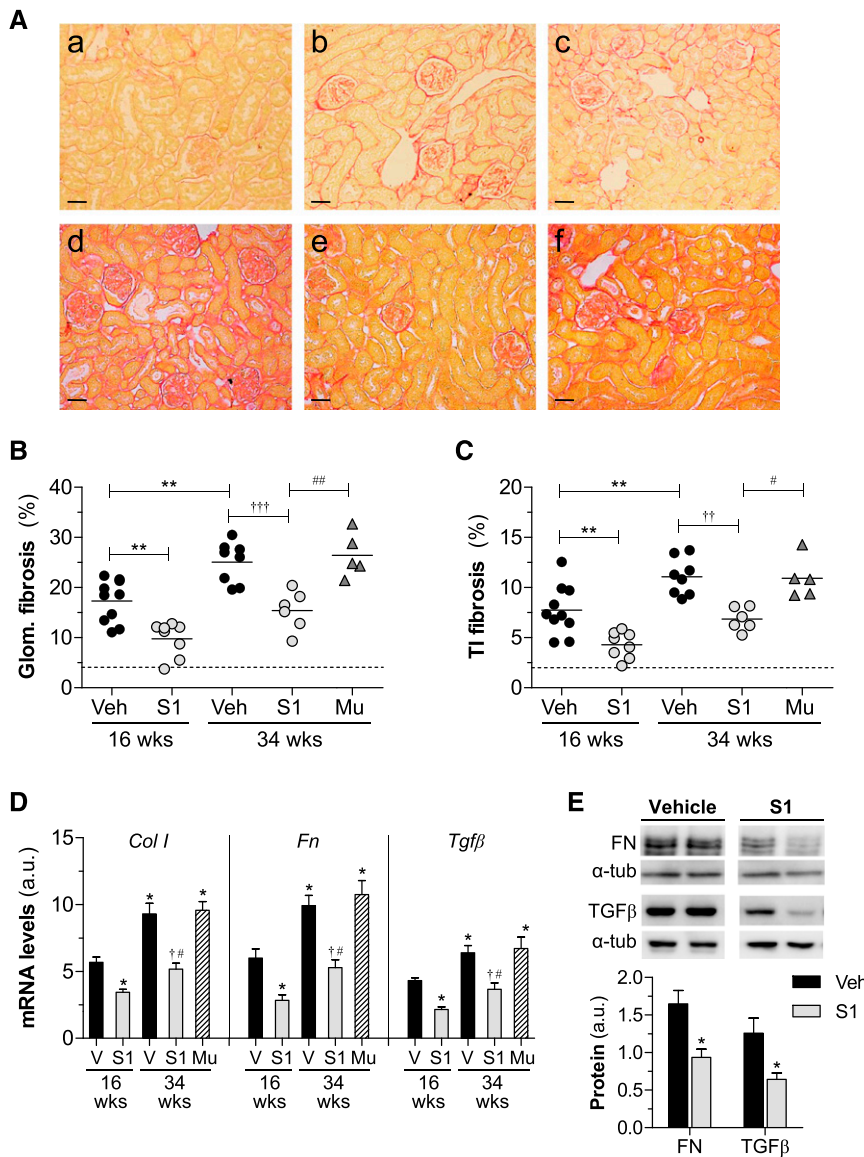


Figure 3. Effect of SOCS1 peptide on diabetes-induced renal fibrosis. (A) Representative images of picosirius red–sensitive collagen staining in renal sections from mice in the early (age 16 weeks; a–c) and late (age 34 weeks; d–f) diabetes models: nondiabetes (a), diabetes+vehicle (b and d), diabetes+S1 (c and e) and diabetes+Mu (f). Quantification of fibrosis (% picosirius red area) in glomerular (Glom.) (B) and tubulointerstitial (TI) (C) compartments. Horizontal dotted lines represent the mean values for nondiabetic mice. (D) Real-time PCR analysis of type I collagen (*Col 1*), fibronectin (*Fn*), and *Tgfb* in renal cortex. Normalized values are expressed in arbitrary units (a.u.). (E) Western blot analyses of fibronectin (FN) and TGFβ expression in renal cortical lysates from diabetic mice. Shown are representative blots and the summary of normalized densitometric quantification. Bars represent the mean±SEM of 5–10 animals per group. Veh/V, vehicle. **P*<0.05 and ***P*<0.01 versus Veh (16 weeks); †*P*<0.05, ††*P*<0.01, and †††*P*<0.001 versus Veh (34 weeks); #*P*<0.05 and ###*P*<0.01 versus Mu. Original magnification, ×100 in A.

genes, growth factors, and extracellular matrix proteins.^{7,17–19} Consistent with previous studies in renal biopsies from patients with early and progressive DN,^{14,20,21} our results in a well established model of combined hyperglycemia and

hyperlipidemia (diabetic apoE-deficient mice) demonstrate that enhanced expression/activation of STAT1/3 and decreased SOCS1 expression are associated with the duration of diabetes, thus confirming the key role of the JAK/STAT/SOCS axis in the pathogenesis of DN. Remarkably, this is the first evidence of a successful and safe peptide-based approach for the specific inhibition of JAK/STAT-mediated responses in DN. This adds to the list of emerging inhibitors of JAKs (AG-490, tofacitinib, baricitinib, Janex-1) and STATs (fludarabine, antisense oligonucleotides) that improve renal damage in experimental models,^{22–26} among which only baricitinib is under clinical evaluation in diabetes.^{5,8}

The SOCS family stands at the crossroad of multiple signaling mechanisms and has emerged as an interesting therapeutic target with anti-inflammatory actions.^{10,11,13} In particular, SOCS1/3 expression pattern is altered in inflammatory diseases^{12,18,27,28} and correlates with cardiovascular risk and progressive loss of renal function in CKD.^{29,30} Our reports in diabetic patients and animals^{17,31} proposed SOCS1 induction as a compensatory mechanism not sufficient to suppress JAK/STAT overactivation in renal disease. Accordingly, SOCS1 gene therapy using local and systemic delivery routes mitigates proteinuria, renal inflammation, and fibrosis in diabetic mice.^{19,31,32} However, gene therapy limitations (*e.g.*, transfection efficiency, duration, and vector toxicity) are critical for long-term use in chronic diseases. Alternative technologies such as peptide drugs have gained interest as therapeutics, with approximately 140 peptides currently in clinical trials.³³ In this regard, several mimetic/antagonist peptides targeting JAK/STAT/SOCS axis are under preclinical evaluation as immunomodulators.^{34,35}

Given the importance of SOCS1 in regulating the JAK/STAT-mediated activities of diabetic factors, we have studied the renal effects of a peptidomimetic of SOCS1 KIR region. This sequence has been shown to inhibit all four JAKs by binding to the activation loop (JAK2 residues 1001–1013), thus suppressing STAT activation independently of SOCS box-mediated proteasomal degradation.³⁶ Consistent with our previous findings that SOCS1 peptide is easily synthesized, tends to adopt an α-helical structure, and becomes

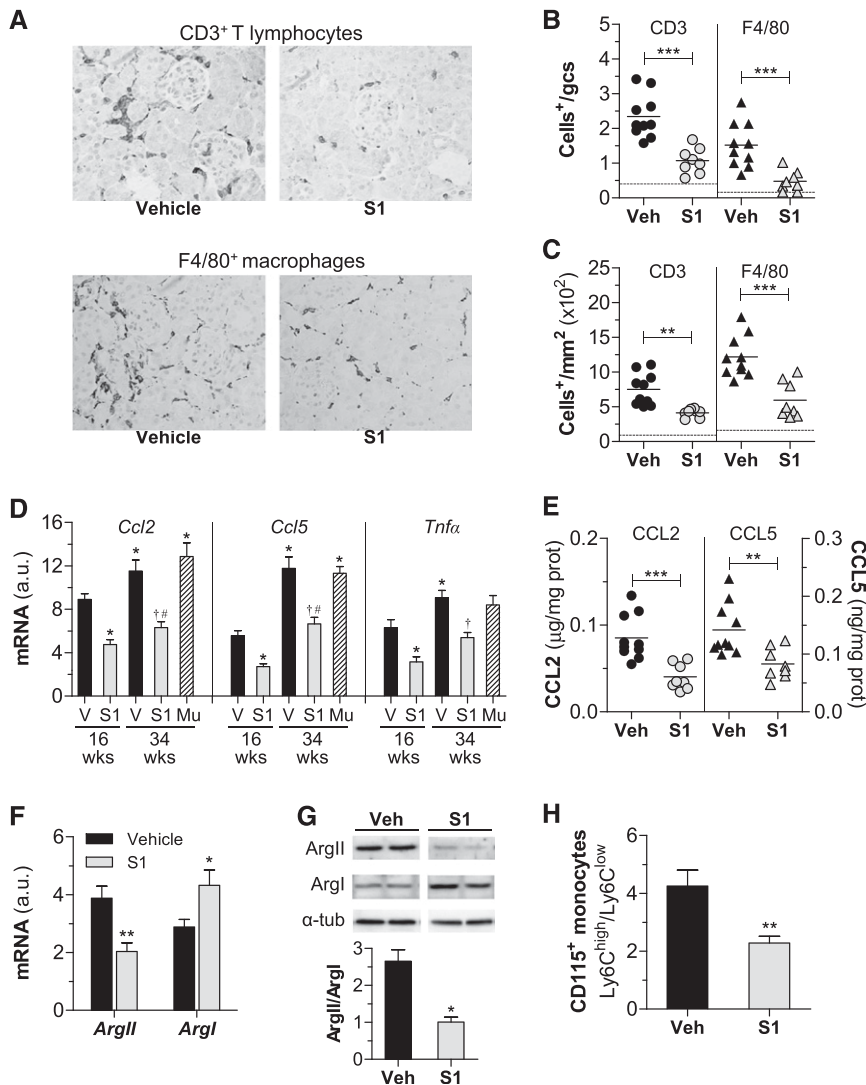


Figure 4. SOCS1 peptide decreases inflammation in diabetic mice. (A–C) Histologic analysis of T lymphocytes and macrophages in kidney sections from diabetic mice (early model). (A) Representative micrographs. Quantification of CD3⁺ and F4/80⁺ cells in glomeruli (B) and interstitium (C). Horizontal dotted lines represent the mean values for nondiabetic mice. (D) Real-time PCR analysis of inflammatory genes in renal cortex. Normalized values are expressed in arbitrary units (a.u.). (E) Kidney chemokine levels measured by ELISA. (F) Gene expression levels of arginase isoforms (ArgII and ArgI) in diabetic kidneys. Real-time PCR data normalized by 18S are expressed in a.u. (G) Representative immunoblots and summary of the relative levels of ArgII and ArgI protein expression in renal lysates from diabetic mice. (H) Flow cytometry analysis of relative CD115⁺ monocyte population (Ly6C^{high} and Ly6C^{low}) in peripheral blood. Bars represent the mean ± SEM of 5–10 animals per group. Veh/V, vehicle. *P < 0.05, **P < 0.01, and ***P < 0.001 versus Veh (16 weeks); †P < 0.05 versus Veh (34 weeks); #P < 0.05 versus Mu. Original magnification, ×200 in A.

cell-permeable and proteolytically stable by N-terminal palmitoylation,²⁰ we show here efficient peptide delivery into renal cells, *in vivo* and *in vitro*, and cytoplasmic localization. Internalized peptide further suppressed STAT1/3 activation, reduced the expression of a broad range of mediators

induced by hyperglycemic and inflammatory conditions, and also prevented cell proliferation and migration processes without affecting cell viability. By contrast, a phenylalanine-substituted analog peptide failed to block STAT activation and cell responses to cytokines, which is compatible with previously identified KIR critical residues (Phe56 and Phe59) for JAK inhibition.^{12,13}

Different SOCS-like molecules have been reported to dampen cytokine receptor activities and further downstream signal transduction events in cancer cells, leukocytes, keratinocytes, and smooth muscle cells.^{20,36–40} *In vivo*, SOCS-derived peptides improve outcome in experimental multiple sclerosis, peripheral nerve injury, and infection.^{35,36,38–40} Likewise, and consistent with our previous findings on the atheroprotective effect of SOCS1,^{20,41} this study demonstrates that a SOCS1 peptidomimetic suppresses STAT1/3 activation in diabetic kidneys and retards development and progression of experimental DN. These effects occur independently of improved glucose control and lipid profile, suggesting the use of SOCS1 peptide in diabetic complications rather than in the disease process.

Diabetes-associated inflammation promotes a progressive accumulation of T cells and macrophages in the kidney, which further contribute to diabetic renal injury either by direct interaction/activation of intrinsic renal cells or by releasing proinflammatory and profibrotic factors involved in cell proliferation, migration, and fibrosis.^{3,42} Our study demonstrates that systemic administration of SOCS1 peptide in diabetic mice improved renal function parameters (serum creatinine and UAC) and glomerular lesions (hypertrophy, mesangial expansion, glomerulosclerosis, and infiltrating T lymphocytes and macrophages) without any observable toxicity. SOCS1-treated mice were also protected from the development of tubular atrophy and interstitial fibrosis and inflammation. These obser-

variations, in conjunction with a reduced expression of cytokines, growth factors, and extracellular matrix proteins suggest that SOCS1 peptide effectively attenuated renal inflammation and fibrosis, two hallmarks of progressive renal disease.¹⁶

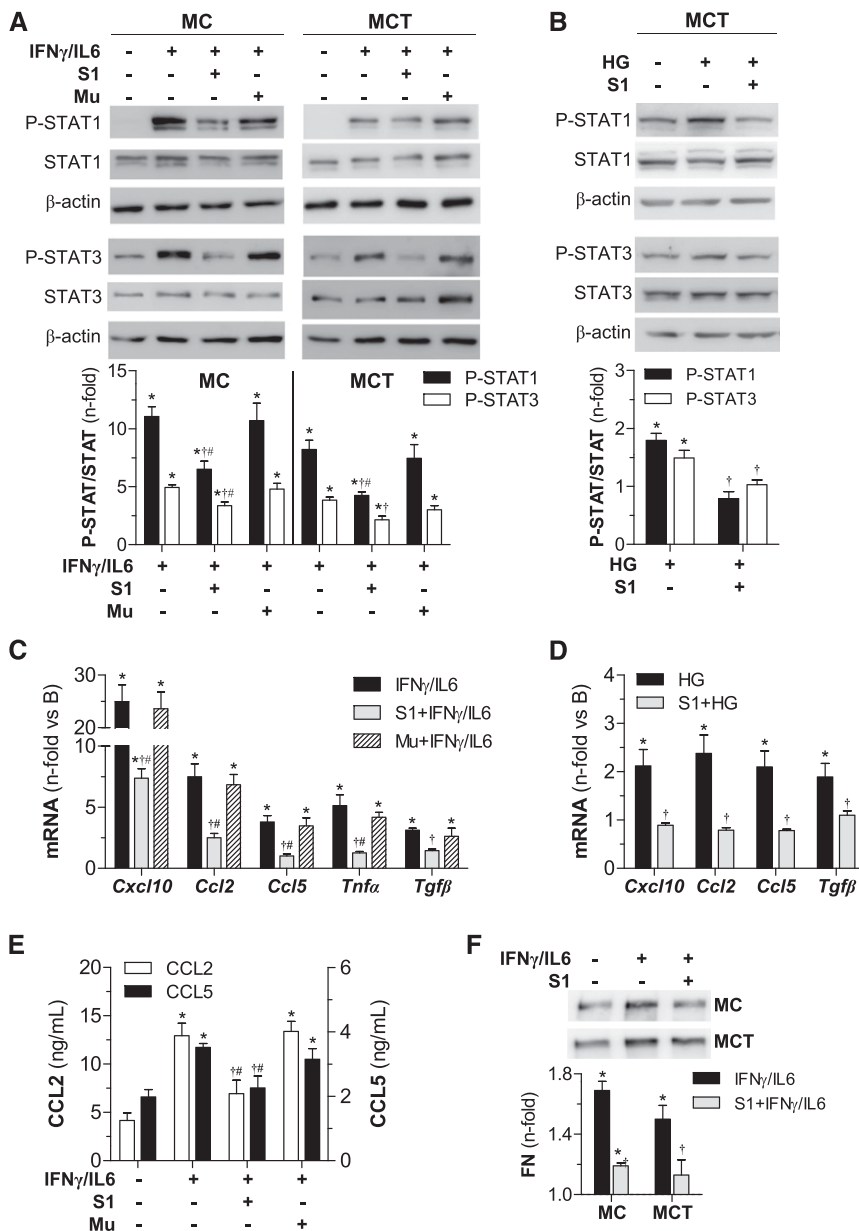


Figure 5. SOCS1 peptide inhibits STAT activation and target gene expression *in vitro*. Western blot analysis for P-STAT1 and P-STAT3 proteins in total cell extracts from MC and MCT stimulated with cytokines (60 minutes) (A) and HG (6 hours) (B) in the presence or absence of peptides (100 μ g/ml). Representative immunoblots are shown and densitometry data expressed as fold increases over basal conditions (arbitrarily set to 1). Real-time PCR analysis of indicated genes in MCT at 24 hours of stimulation with cytokines (C) and HG (D). (E) CCL2 and CCL5 concentrations in MC supernatants measured by ELISA. (F) Western blot of fibronectin (FN) levels in culture supernatants. Bars represent the mean \pm SEM of 4–7 independent experiments. * P <0.05 versus basal; $\dagger P$ <0.05 versus stimulus; # P <0.05 versus Mu.

The heterogeneity of macrophage phenotype and function ultimately determines the outcome of DN.⁴³ The majority of kidney injury–associated macrophages are derived from a subset of recruited “inflammatory” monocytes (Ly6C^{high}-expressing in mice) which then undergo differentiation into: (1) classically

activated M1 macrophages mediating inflammation and tissue damage, or (2) alternatively activated M2 macrophages mainly involved in renal tissue repair.⁴³ We observed that SOCS1 peptide reduced circulating Ly6C^{high} monocytes and kidney-infiltrating M1 macrophages, which is compatible with the reported function of SOCS1 as a negative regulator of M1 inflammatory responses.⁴⁴

Evidence indicates a complex role for SOCS family in the pathophysiology of diabetes. In type 1 diabetes, SOCS1 overexpression improves hyperglycemia-induced β cell damage and prevents diabetes development in nonobese mice.^{45,46} In type 2 diabetes, SOCS1 protects mice against systemic inflammation⁴⁷ and prevents high fat–induced insulin resistance⁴⁸ but, paradoxically, SOCS1 inhibition ameliorates insulin resistance and metabolic syndrome in obese diabetic db/db mice.⁴⁹ It has been reported that SOCS1 can disturb insulin signaling by targeting receptor and adapter proteins for proteasomal degradation, thus contributing to glucose intolerance and insulin resistance.⁵⁰ Unlike whole protein, our SOCS1 peptide lacks the conserved SOCS box required to promote degradation of insulin-signaling proteins, which may explain its renoprotective effect in diabetic mice without affecting glucose metabolism.

Collectively, this study emphasizes the pivotal role of the JAK/STAT/SOCS axis in regulating proinflammatory and profibrotic factors in the diabetic kidney, and proposes SOCS1 peptidomimetic as a useful approach to dampen renal inflammation and fibrosis, thus decreasing albuminuria and preserving renal function during the course of DN.

CONCISE METHODS

A complete description of the methods are available in Supplemental Material.

Diabetes Mouse Model and Treatments

Animal studies conformed to the Directive 2010/63/EU of the European Parliament and were approved by the Institutional Animal Care and Use Committee (IIS-Fundacion Jimenez Diaz). Diabetes was induced in male apoE-deficient mice by consecutive intraperitoneal streptozotocin injections (125 mg/kg per day for 2 days).^{15,41} Diabetic mice (glycemia \geq 19.4 mmol/L) were

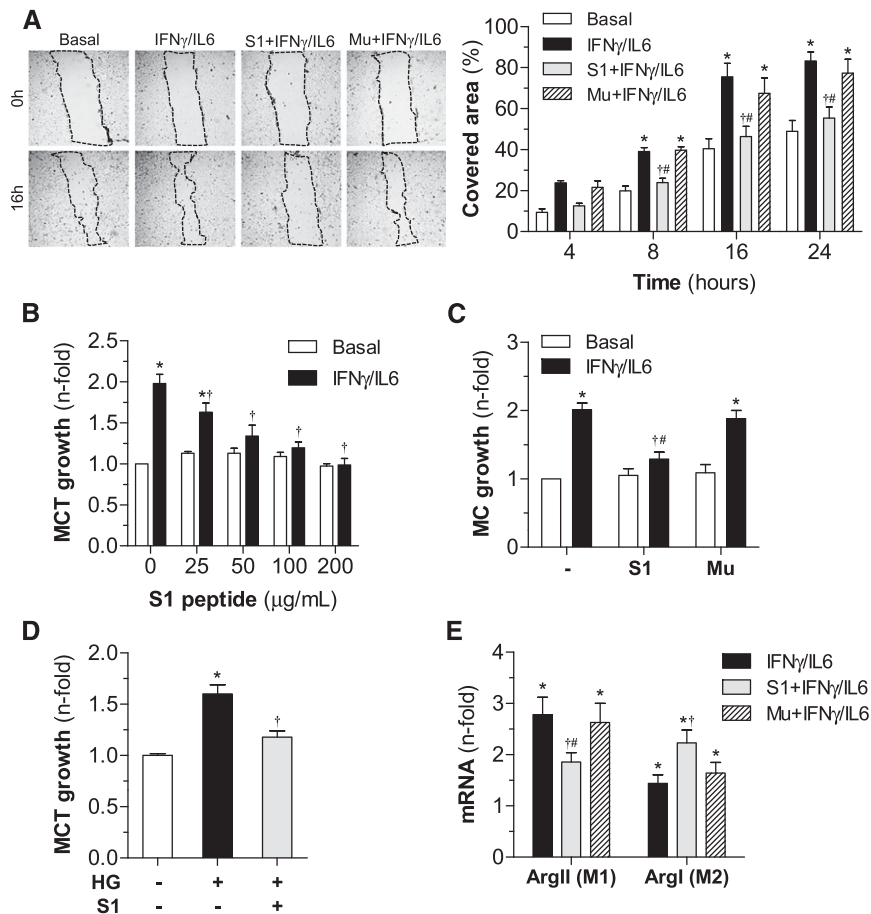


Figure 6. *In vitro* effects of SOCS1 peptide on cell migration, proliferation, and differentiation. (A) Analysis of MC migration by scratch-wound-healing assay. Representative phase-contrast images of cells migrating into the wounded area (dotted lines) at 0 hours and 16 hours of cytokine incubation in the absence or presence of peptides (S1 and Mu sequences, 100 $\mu\text{g}/\text{ml}$). The graph shows the results from quantification of covered healing areas over time. (B) Dose-dependent curves of peptides on cell viability (basal conditions) and proliferation (cytokine stimulation) in MCT (MTT assay, 48 hours). (C) Effect of peptides (100 $\mu\text{g}/\text{ml}$) on MC growth. (D) Antiproliferative effect of S1 peptide on HG-stimulated MCT. (E) Real-time PCR analysis of arginase isoforms (ArgII and ArgI) in bone marrow–derived macrophages. Data expressed as percentage or fold increases over basal conditions are mean \pm SEM ($n=4-6$ experiments). * $P<0.05$ versus basal; † $P<0.05$ versus stimulus; # $P<0.05$ versus Mu.

randomized to receive vehicle ($n=18$), SOCS1 peptide ($n=14$), or mutant inactive peptide ($n=5$) intraperitoneally once every second day for a total of 6–10 weeks starting at 10 weeks of age (early treatment) or at 24 weeks of age (late treatment) (Supplemental Figure 3A). Age-matched nondiabetic mice ($n=5$) were used as controls.

At the end of the study, blood samples were collected for biochemistry and flow cytometry; urine samples for UAC calculation; and dissected kidneys for histology, RNA, and protein expression. Histologic scoring (0–3 scale), glomerular size, and mesangial area were quantified in PAS-stained paraffin sections. Collagen content was examined by picrosirius red staining. Macrophages (F4/80), T lymphocytes (CD3), and STAT proteins were detected by immunoperoxidase. Positive staining was expressed as percentage of total area

and number of positive cells (per glomerular cross-section [gcs] or per mm^2).

In Vitro Studies

Mouse glomerular MC, tubular MCT, and bone marrow–derived macrophages were treated for 90 minutes with peptides (S1 and Mu sequences) before stimulation with cytokines (10^3 U/ml IFN γ plus 10^2 U/ml IL-6) or HG (30 mmol/L D-glucose). Gene and protein expressions were analyzed by real-time PCR, Western blot, and ELISA. Cell migration and proliferation/viability were assessed by *in vitro* wound healing and 3-(4, 5-dimethylthiazol-2-yl)-2, 5-diphenyltetrazolium bromide (MTT) assay.⁴¹

Statistical Analyses

Results are presented as individual data points and mean \pm SEM of duplicate/triplicate determinations. Differences across groups were considered significant at $P<0.05$ (ANOVA with the Bonferroni *post hoc* test). Pearson correlation analyses were performed for normally distributed parameters.

ACKNOWLEDGMENTS

The authors greatly acknowledge the initial contributions of Dr. B. Mallavia and J. Calavia (Fundacion Jimenez Diaz University Hospital-Health Research Institute) to the animal models and cellular studies. We also thank Dr. L.M. Blanco-Colio and V. Fernandez-Laso for their help with silencing experiments. C.R. and C.G. G. designed the study, researched and analyzed data, and wrote the manuscript. I.L. and A.O. designed the experiments, analyzed data, and critically revised the manuscript. L.L.S. and S.B. evaluated *in vivo* and *in vitro* data. J.E. and J.B.

analyzed or interpreted data and reviewed the manuscript for intellectual content. C.G.G. is the guarantor of this work.

This work was supported by the Spanish Ministry of Economy and Competitiveness (SAF2012-38830, SAF2015-63696-R), European Regional Development Fund-Ministry of Health (PI14/00386, PIE13/00051), a European Union–funded program (“KidneyConnect”), the Iñigo Alvarez de Toledo Renal Foundation, the Conchita Rabago Foundation, and the Spanish Societies of Nephrology and Arteriosclerosis.

The results included in this paper are under the protection of a patent issued by our institutions (Fundacion Jimenez Diaz University Hospital-Health Research Institute and Autonoma University of Madrid).

DISCLOSURES

C.G.G. and J.E. are inventors on a patent application regarding peptide. The other authors declare no conflict of interest.

REFERENCES

1. Fineberg D, Jandeleit-Dahm KA, Cooper ME: Diabetic nephropathy: diagnosis and treatment. *Nat Rev Endocrinol* 9: 713–723, 2013
2. Wada J, Makino H: Inflammation and the pathogenesis of diabetic nephropathy. *Clin Sci (Lond)* 124: 139–152, 2013
3. Navarro-González JF, Mora-Fernández C, Muros de Fuentes M, García-Pérez J: Inflammatory molecules and pathways in the pathogenesis of diabetic nephropathy. *Nat Rev Nephrol* 7: 327–340, 2011
4. Tuttle KR, Bakris GL, Bilous RW, Chiang JL, de Boer IH, Goldstein-Fuchs J, Hirsch IB, Kalantar-Zadeh K, Narva AS, Navaneethan SD, Neumiller JJ, Patel UD, Ratner RE, Whaley-Connell AT, Molitch ME: Diabetic kidney disease: a report from an ADA Consensus Conference. *Diabetes Care* 37: 2864–2883, 2014
5. Fernandez-Fernandez B, Ortiz A, Gomez-Guerrero C, Egido J: Therapeutic approaches to diabetic nephropathy—beyond the RAS. *Nat Rev Nephrol* 10: 325–346, 2014
6. Marrero MB, Banes-Berceli AK, Stern DM, Eaton DC: Role of the JAK/STAT signaling pathway in diabetic nephropathy. *Am J Physiol Renal Physiol* 290: F762–F768, 2006
7. Matsui F, Meldrum KK: The role of the Janus kinase family/signal transducer and activator of transcription signaling pathway in fibrotic renal disease. *J Surg Res* 178: 339–345, 2012
8. Brosius FC 3rd, He JC: JAK inhibition and progressive kidney disease. *Curr Opin Nephrol Hypertens* 24: 88–95, 2015
9. Stark GR, Darnell JE Jr: The JAK-STAT pathway at twenty. *Immunity* 36: 503–514, 2012
10. Kiu H, Nicholson SE: Biology and significance of the JAK/STAT signalling pathways. *Growth Factors* 30: 88–106, 2012
11. Yoshimura A, Naka T, Kubo M: SOCS proteins, cytokine signalling and immune regulation. *Nat Rev Immunol* 7: 454–465, 2007
12. Trengove MC, Ward AC: SOCS proteins in development and disease. *Am J Clin Exp Immunol* 2: 1–29, 2013
13. Linossi EM, Babon JJ, Hilton DJ, Nicholson SE: Suppression of cytokine signaling: the SOCS perspective. *Cytokine Growth Factor Rev* 24: 241–248, 2013
14. Berthier CC, Zhang H, Schin M, Henger A, Nelson RG, Yee B, Boucherot A, Neusser MA, Cohen CD, Carter-Su C, Argetsinger LS, Rastaldi MP, Brosius FC, Kretzler M: Enhanced expression of Janus kinase-signal transducer and activator of transcription pathway members in human diabetic nephropathy. *Diabetes* 58: 469–477, 2009
15. Lopez-Parra V, Mallavia B, Lopez-Franco O, Ortiz-Muñoz G, Oguiza A, Recio C, Blanco J, Nimmerjahn F, Egido J, Gomez-Guerrero C: Fcγ receptor deficiency attenuates diabetic nephropathy. *J Am Soc Nephrol* 23: 1518–1527, 2012
16. Boor P, Floege J: Chronic kidney disease growth factors in renal fibrosis. *Clin Exp Pharmacol Physiol* 38: 441–450, 2011
17. Hernández-Vargas P, López-Franco O, Sanjuán G, Rupérez M, Ortiz-Muñoz G, Suzuki Y, Aguado-Roncero P, Pérez-Tejerizo G, Blanco J, Egido J, Ruiz-Ortega M, Gómez-Guerrero C: Suppressors of cytokine signaling regulate angiotensin II-activated Janus kinase-signal transducers and activators of transcription pathway in renal cells. *J Am Soc Nephrol* 16: 1673–1683, 2005
18. Ortiz-Muñoz G, Martin-Ventura JL, Hernandez-Vargas P, Mallavia B, Lopez-Parra V, Lopez-Franco O, Muñoz-García B, Fernandez-Vizarrá P, Ortega L, Egido J, Gomez-Guerrero C: Suppressors of cytokine signaling modulate JAK/STAT-mediated cell responses during atherosclerosis. *Arterioscler Thromb Vasc Biol* 29: 525–531, 2009
19. Shi Y, Du C, Zhang Y, Ren Y, Hao J, Zhao S, Yao F, Duan H: Suppressor of cytokine signaling-1 ameliorates expression of MCP-1 in diabetic nephropathy. *Am J Nephrol* 31: 380–388, 2010
20. Recio C, Oguiza A, Lazaro I, Mallavia B, Egido J, Gomez-Guerrero C: Suppressor of cytokine signaling 1-derived peptide inhibits Janus kinase/signal transducers and activators of transcription pathway and improves inflammation and atherosclerosis in diabetic mice. *Arterioscler Thromb Vasc Biol* 34: 1953–1960, 2014
21. Hodgin JB, Nair V, Zhang H, Randolph A, Harris RC, Nelson RG, Weil EJ, Cavalcoli JD, Patel JM, Brosius FC 3rd, Kretzler M: Identification of cross-species shared transcriptional networks of diabetic nephropathy in human and mouse glomeruli. *Diabetes* 62: 299–308, 2013
22. Wang X, Shaw S, Amiri F, Eaton DC, Marrero MB: Inhibition of the Jak/STAT signaling pathway prevents the high glucose-induced increase in tgf-beta and fibronectin synthesis in mesangial cells. *Diabetes* 51: 3505–3509, 2002
23. Tang SC, Leung JC, Chan LY, Tsang AW, Lai KN: Activation of tubular epithelial cells in diabetic nephropathy and the role of the peroxisome proliferator-activated receptor-gamma agonist. *J Am Soc Nephrol* 17: 1633–1643, 2006
24. Chen J, Feigenbaum L, Awasthi P, Butcher DO, Anver MR, Golubeva YG, Bamford R, Zhang X, St Claire MB, Thomas CJ, Discepolo V, Jabri B, Waldmann TA: Insulin-dependent diabetes induced by pancreatic beta cell expression of IL-15 and IL-15Rα. *Proc Natl Acad Sci U S A* 110: 13534–13539, 2013
25. Khan IM, Perrard XY, Brunner G, Lui H, Sparks LM, Smith SR, Wang X, Shi ZZ, Lewis DE, Wu H, Ballantyne CM: Intermuscular and perimuscular fat expansion in obesity correlates with skeletal muscle T cell and macrophage infiltration and insulin resistance. *Int J Obes* 39: 1607–1618, 2015
26. Cetkovic-Cvrlje M, Dragt AL, Vassilev A, Liu XP, Uckun FM: Targeting JAK3 with JANEX-1 for prevention of autoimmune type 1 diabetes in NOD mice. *Clin Immunol* 106: 213–225, 2003
27. Liang X, He M, Chen T, Liu Y, Tian YL, Wu YL, Zhao Y, Shen Y, Yuan ZY: Multiple roles of SOCS proteins: differential expression of SOCS1 and SOCS3 in atherosclerosis. *Int J Mol Med* 31: 1066–1074, 2013
28. Sasi W, Jiang WG, Sharma A, Mokbel K: Higher expression levels of SOCS 1,3,4,7 are associated with earlier tumour stage and better clinical outcome in human breast cancer. *BMC Cancer* 10: 178, 2010
29. Rastmanesh MM, Bluysen HA, Joles JA, Boer P, Willekes N, Braam B: Increased expression of SOCS3 in monocytes and SOCS1 in lymphocytes correlates with progressive loss of renal function and cardiovascular risk factors in chronic kidney disease. *Eur J Pharmacol* 593: 99–104, 2008
30. Neuwirt H, Eder IE, Pühr M, Rudnicki M: SOCS-3 is downregulated in progressive CKD patients and regulates proliferation in human renal proximal tubule cells in a STAT1/3 independent manner. *Lab Invest* 93: 123–134, 2013
31. Ortiz-Muñoz G, Lopez-Parra V, Lopez-Franco O, Fernandez-Vizarrá P, Mallavia B, Flores C, Sanz A, Blanco J, Mezzano S, Ortiz A, Egido J, Gomez-Guerrero C: Suppressors of cytokine signaling abrogate diabetic nephropathy. *J Am Soc Nephrol* 21: 763–772, 2010
32. Liu Q, Xing L, Wang L, Yao F, Liu S, Hao J, Liu W, Duan H: Therapeutic effects of suppressors of cytokine signaling in diabetic nephropathy. *J Histochem Cytochem* 62: 119–128, 2014
33. Fosgerau K, Hoffmann T: Peptide therapeutics: current status and future directions. *Drug Discov Today* 20: 122–128, 2015
34. Auzenne EJ, Klostergaard J, Mandal PK, Liao WS, Lu Z, Gao F, Bast RC Jr, Robertson FM, McMurray JS: A phosphopeptide mimetic prodrug targeting the SH2 domain of Stat3 inhibits tumor growth and angiogenesis. *J Exp Ther Oncol* 10: 155–162, 2012
35. Ahmed CM, Larkin J 3rd, Johnson HM: SOCS1 Mimetics and Antagonists: A Complementary Approach to Positive and Negative Regulation of Immune Function. *Front Immunol* 6: 183, 2015

36. Waiboci LW, Ahmed CM, Mujtaba MG, Flowers LO, Martin JP, Haider MI, Johnson HM: Both the suppressor of cytokine signaling 1 (SOCS-1) kinase inhibitory region and SOCS-1 mimetic bind to JAK2 autophosphorylation site: implications for the development of a SOCS-1 antagonist. *J Immunol* 178: 5058–5068, 2007
37. Flowers LO, Subramaniam PS, Johnson HM: A SOCS-1 peptide mimetic inhibits both constitutive and IL-6 induced activation of STAT3 in prostate cancer cells. *Oncogene* 24: 2114–2120, 2005
38. Jager LD, Dabelic R, Waiboci LW, Lau K, Haider MS, Ahmed CM, Larkin J 3rd, David S, Johnson HM: The kinase inhibitory region of SOCS-1 is sufficient to inhibit T-helper 17 and other immune functions in experimental allergic encephalomyelitis. *J Neuroimmunol* 232: 108–118, 2011
39. Madonna S, Scarponi C, Doti N, Carbone T, Cavani A, Scognamiglio PL, Marasco D, Albanesi C: Therapeutic potential of a peptide mimicking the SOCS1 kinase inhibitory region in skin immune responses. *Eur J Immunol* 43: 1883–1895, 2013
40. Mujtaba MG, Flowers LO, Patel CB, Patel RA, Haider MI, Johnson HM: Treatment of mice with the suppressor of cytokine signaling-1 mimetic peptide, tyrosine kinase inhibitor peptide, prevents development of the acute form of experimental allergic encephalomyelitis and induces stable remission in the chronic relapsing/remitting form. *J Immunol* 175: 5077–5086, 2005
41. Recio C, Oguiza A, Mallavia B, Lazaro I, Ortiz-Muñoz G, Lopez-Franco O, Egido J, Gomez-Guerrero C: Gene delivery of suppressors of cytokine signaling (SOCS) inhibits inflammation and atherosclerosis development in mice. *Basic Res Cardiol* 110: 8, 2015
42. Galkina E, Ley K: Leukocyte recruitment and vascular injury in diabetic nephropathy. *J Am Soc Nephrol* 17: 368–377, 2006
43. Ricardo SD, van Goor H, Eddy AA: Macrophage diversity in renal injury and repair. *J Clin Invest* 118: 3522–3530, 2008
44. Whyte CS, Bishop ET, Rückerl D, Gaspar-Pereira S, Barker RN, Allen JE, Rees AJ, Wilson HM: Suppressor of cytokine signaling (SOCS)1 is a key determinant of differential macrophage activation and function. *J Leukoc Biol* 90: 845–854, 2011
45. Chong MM, Chen Y, Darwiche R, Dudek NL, Irawaty W, Santamaria P, Allison J, Kay TW, Thomas HE: Suppressor of cytokine signaling-1 overexpression protects pancreatic beta cells from CD8+ T cell-mediated autoimmune destruction. *J Immunol* 172: 5714–5721, 2004
46. Suchy D, Łabuzek K, Machnik G, Kozłowski M, Okopień B: SOCS and diabetes—ups and downs of a turbulent relationship. *Cell Biochem Funct* 31: 181–195, 2013
47. Sachithanandan N, Graham KL, Galic S, Honeyman JE, Fynch SL, Hewitt KA, Steinberg GR, Kay TW: Macrophage deletion of SOCS1 increases sensitivity to LPS and palmitic acid and results in systemic inflammation and hepatic insulin resistance. *Diabetes* 60: 2023–2031, 2011
48. Emanuelli B, Macotela Y, Boucher J, Ronald Kahn C: SOCS-1 deficiency does not prevent diet-induced insulin resistance. *Biochem Biophys Res Commun* 377: 447–452, 2008
49. Ueki K, Kondo T, Tseng YH, Kahn CR: Central role of suppressors of cytokine signaling proteins in hepatic steatosis, insulin resistance, and the metabolic syndrome in the mouse. *Proc Natl Acad Sci U S A* 101: 10422–10427, 2004
50. Rui L, Yuan M, Frantz D, Shoelson S, White MF: SOCS-1 and SOCS-3 block insulin signaling by ubiquitin-mediated degradation of IRS1 and IRS2. *J Biol Chem* 277: 42394–42398, 2002

This article contains supplemental material online at <http://jasn.asnjournals.org/lookup/suppl/doi:10.1681/ASN.2016020237/-/DCSupplemental>.

COMPLETE METHODS

Suppressor of cytokine signaling-1 (SOCS1) peptidomimetic limits progression of diabetic nephropathy

C. Recio, I. Lazaro, A. Oguiza, L. Lopez-Sanz, S. Bernal, J. Blanco, J. Egido, and C. Gomez-Guerrero.

Peptide synthesis

Palmitoylated peptides derived from mouse SOCS1 KIR sequence^{1,2} (residues 53-68; mutant inactive F→A) were synthesized and rhodamin-labeled (ProteoGenix), then dissolved in 1% DMSO in saline solution and filter-sterilized.

Diabetes model and treatments

All animal studies were performed according to the Directive 2010/63/EU of the European Parliament and were approved by the Institutional Animal Care and Use Committee (IIS-Fundacion Jimenez Diaz). Experimental diabetes model of insulin deficiency^{2,3} was induced in male Apolipoprotein E (ApoE)-deficient mice (Jackson Laboratory) by two daily intraperitoneal injections of streptozotocin (STZ, 125 mg/kg/day; Sigma-Aldrich) in 10 mmol/L citrate buffer. Animals maintained on standard diet were monitored every 2-3 days for body weight and non-fasting blood glucose (glucometer strips). Diabetes was defined as blood glucose >19.4 mmol/L. Severely hyperglycemic mice (glucose >29 mmol/L) were given subcutaneous intermittent low dosages of long acting insulin (1–1.5 IU) to maintain blood glucose levels within a more tolerable range^{3,4}.

In a first experiment (early model), 8-week-old mice (n=18) were made diabetic and after 2 weeks of STZ injection were randomized to receive either vehicle (0.1% DMSO in saline solution, 200µL; n=10) or SOCS1-derived peptide (65 µg/day in 200µL; n=8) administered intraperitoneally every second day for 6 weeks. Age-matched non-diabetic mice (n=5) receiving citrate buffer alone were used as control.

In a parallel experiment (late model), 22-week-old ApoE mice (n=19) were made diabetic and after 2 weeks of STZ injection were treated with vehicle (0.1% DMSO in saline solution, 200µL; n=8), SOCS1 peptide (65 µg/day in 200µL; n=6), and mutant inactive peptide (65 µg/day in 200µL; n=5) administered intraperitoneally every second day for additional 10 weeks.

Clinical signs of toxicity related to treatment such as weight gain/loss, abnormal behavior, discoloration of urine, stool and fur were monitored throughout the studies.

At 16 and 34 weeks of age, 16 hour-fasted mice were anesthetized (100 mg/kg ketamine and 15 mg/kg xylazine) and saline perfused. After collection of blood and urine samples, the mice were killed and kidneys were harvested, then snap-frozen for RNA/protein expression studies or stored in 4% paraformaldehyde for histology.

Biodistribution and pharmacokinetics

For localization experiments, mice received a single intraperitoneal injection of rhodamine-labeled SOCS1 peptide, then sacrificed at 0, 3, 6, 16 and 24 h after injection (n=3 animals each time point). The liver, kidneys and spleen were removed and immediately frozen until analysis. Tissue biodistribution was evaluated *ex vivo* by confocal microscopy. Additionally, fluorescence intensity in homogenized samples was measured ($\lambda_{\text{emission}}=540\text{nm}$; $\lambda_{\text{excitation}}=570\text{nm}$) and data normalized to the weight of organ/tissue.

For pharmacokinetics, fluorescence in plasma and urine samples taken at different time points (0.5, 1, 2, 3, 4, 6, 8, 16, 20 and 24 h; n=2 each) was measured. Plasma fluorescence data versus time were plotted, and the data were fitted into a straight line to calculate the plasma half-life of peptide.

Blood and urine determinations

Serum concentrations of total cholesterol, LDL, HDL and triglyceride were determined by autoanalyzer. ELISA kits were used to measure glycated hemoglobin A1c (Gentaur) and urine albumin (Cell Trend). Serum and urine creatinine values were determined by creatininase enzymatic method (Abcam). Single-cell suspensions from EDTA-buffered blood were treated with erythrocyte lysis buffer, then stained with antibodies to CD115 and Ly6C (eBioscience) and analyzed by flow cytometry^{5,6}.

Histology and immunohistochemistry

Paraffin-embedded kidney sections (3 μm) were stained with periodic acid-Schiff (PAS) to evaluate renal pathology. Renal lesions were and blindly graded (0-3 scale) according to the extent of glomerular changes (hypertrophy, hypercellularity, mesangial expansion and capillary dilation; 30 glomeruli), tubular lesions (atrophy and degeneration; 20 fields at 40X magnification), and interstitial damage (fibrosis and infiltration; 20 fields at 40X magnification)^{3,4}. Glomerular area and PAS⁺ mesangial area were quantified by a computerized image analysis system (MetaMorph; Molecular Devices). Collagen content was examined by picrosirius red staining. Immunodetection of phosphorylated STAT1 (P-STAT1 (Tyr701); Invitrogen), phosphorylated STAT3 (P-STAT3 (Ser727); Cell Signaling), macrophages (F4/80; Serotec) and T lymphocytes (CD3; DAKO) was performed by indirect immunoperoxidase technique. Positive staining (>20 fields at 20X magnification; 2-3 tissue slices/mice) were quantified using Image Pro-Plus analysis software (Media Cybernetics), and positive area was expressed as percentage of total area. P-STAT⁺, F4/80⁺ and CD3⁺ cells were expressed as number per glomerular cross-section and number of interstitial cells per mm^2 .

Cell cultures

The murine mesangial cell line SV40 MES 13 (CRL-1927; American Type Culture Collection) was maintained in 3:1 mixture of DMEM and Ham's F12 medium containing 14 mmol/L HEPES and 5% FBS (Life Technologies). The murine proximal tubuloepithelial MCT line^{4,7} was cultured in RPMI 1640 containing 10% FBS. Bone marrow-derived macrophages were cultured for 7 days in DMEM with 10%

FBS and supplemented with 10% L929-cell conditioned medium as a source of macrophage colony stimulating factor⁵. All culture media were supplemented with 100 U/mL penicillin, 100 µg/mL streptomycin and 2 mmol/L L-glutamine (Life Technologies).

Quiescent cells (24 h in medium without FBS) were treated for 90 min with different peptide concentrations (25-200 µg/mL) before stimulation with murine recombinant cytokines (10³ U/mL IFN γ plus 10² U/mL IL-6; PeproTech) and high-glucose concentration (30 mmol/L D-glucose).

Transfection of small-interfering RNA

MCT cells grown to 60-70% confluence were transfected with 30 nmol/L of small interfering RNA (siRNA) targeting STAT1 or negative control scramble siRNA (Ambion) using Lipofectamine RNAiMAX reagent (Life Technologies)⁴. Transfected cells (silencing efficiency 70%) were pretreated with SOCS1 peptide (100 µg/mL) for 90 min before 16 h of stimulation with high-glucose concentration.

mRNA expression analysis

Total RNA from mouse kidney and cultured cells was extracted with Tryzol (Life Technologies)^{3,7}. Target gene expression (*Stat1*, *Stat3*, *Socs1*, *Kim1*, *Coll*, *Fn*, *Tgfb*, *Tnfa*, *Ccl2*, *Ccl5*, *Cxcl10*, *ArgI* and *ArgII*) was analyzed by real-time quantitative PCR (Applied Biosystem) and normalized to 18S housekeeping gene.

Protein expression analysis

Total proteins from kidney tissue and cultured cells were homogenized in ice-cold buffer containing 1% Triton X-100, 0.5% NP-40 and protease inhibitors. Cell conditioned media were collected for chemokine and fibronectin expression.

Proteins were resolved on SDS-PAGE gels, transferred onto polyvinylidene fluoride membranes and immunoblotted for P-STAT1 (Invitrogen), P-STAT3, STAT3 (Cell Signaling), fibronectin (Millipore Corporation), STAT1, TGF β , arginase I and II (Santa Cruz Biotechnology), using α -tubulin (Sigma-Aldrich) or β -actin (Santa Cruz Biotechnology) as loading controls and peroxidase/biotin conjugated secondary antibodies (Amersham). Immunoblots were quantified using Quantity One software (Bio-Rad Laboratories).

CCL2 levels and CCL5 levels in renal samples and cell supernatants were measured using mouse ELISA kits (BD Biosciences and eBiosciences, respectively).

Immunofluorescence analysis was performed in fixed, permeabilized cells by incubation with P-STAT1 and P-STAT3 antibodies, followed by conjugated secondary antibodies (Alexa Fluor 488; Invitrogen) and nuclear counterstaining (4',6-diamidino-2-phenylindole; Sigma-Aldrich). Images were captured using a confocal fluorescent microscope (Leica).

Cell migration and proliferation assays

Mesangial cell migration was measured by the wound-healing assay^{2,8}. Briefly, cells in a confluent monolayer were serum-depleted, followed by a wound injury using a plastic pipette tip, and then preincubated with peptides before cytokine stimulation. Images were collected during the healing period (0-24 h) using a phase contrast microscope (Nikon), and the remaining wound areas were quantified and normalized to time 0 values.

For cell viability/proliferation studies, cells were maintained for 48 h in culture medium alone (viability) and supplemented with either cytokines or high-glucose (proliferation) in the presence of different peptide concentrations, and then assessed by the 3-(4,5-dimethylthiazol-2-yl)-2,5-diphenyltetrazolium bromide (MTT) colorimetric assay.

Statistical analysis

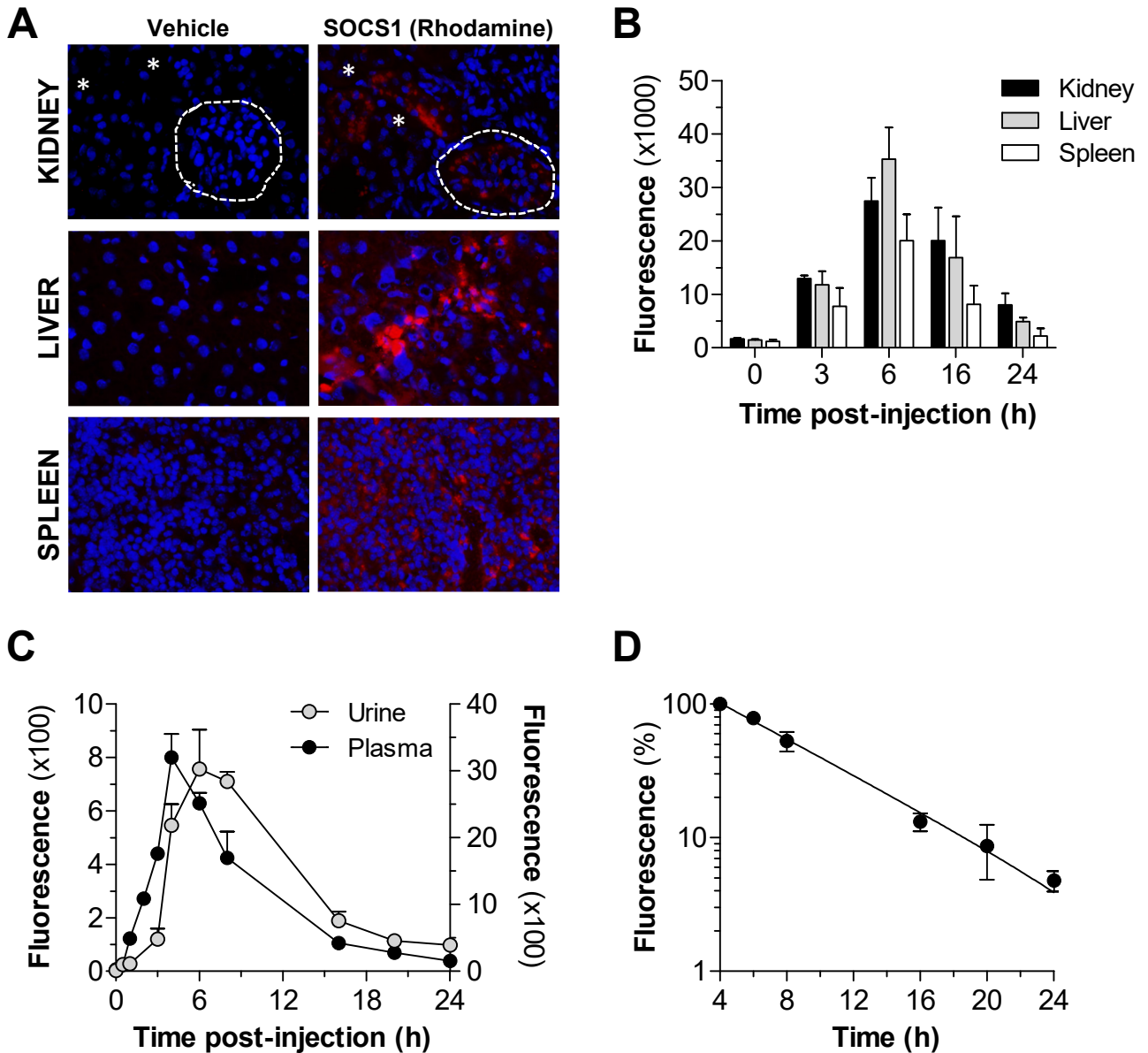
Results are presented as individual data points and mean±SEM. Each experimental condition was analyzed in duplicate/triplicate. Statistical analysis was performed using Prism 5 (GraphPad Software Inc). Data passed the D'Agostino and Pearson omnibus normality test and were tested for homogeneity of variance with the Bartlett test. Pearson's correlation analysis were performed for normally distributed parameters. Differences across groups were considered significant at P<0.05 using either unpaired Student's t test or one-tail ANOVA followed by post-hoc Bonferroni pairwise comparison test.

References

1. Waiboci LW, Ahmed CM, Mujtaba MG, Flowers LO, Martin JP, Haider MI, Johnson HM: Both the suppressor of cytokine signaling 1 (SOCS-1) kinase inhibitory region and SOCS-1 mimetic bind to JAK2 autophosphorylation site: implications for the development of a SOCS-1 antagonist. *J Immunol* 178:5058-5068, 2007
2. Recio C, Oguiza A, Lazaro I, Mallavia B, Egado J, Gomez-Guerrero C: Suppressor of cytokine signaling 1-derived peptide inhibits Janus kinase/signal transducers and activators of transcription pathway and improves inflammation and atherosclerosis in diabetic mice. *Arterioscler Thromb Vasc Biol* 34:1953-1960, 2014
3. Lopez-Parra V, Mallavia B, Lopez-Franco O, Ortiz-Munoz G, Oguiza A, Recio C, Blanco J, Nimmerjahn F, Egado J, Gomez-Guerrero C: Fcγ receptor deficiency attenuates diabetic nephropathy. *J Am Soc Nephrol* 23:1518-1527, 2012
4. Lazaro I, Oguiza A, Recio C, Mallavia B, Madrigal-Matute J, Blanco J, Egado J, Martin-Ventura JL, Gomez-Guerrero C: Targeting HSP90 Ameliorates Nephropathy and Atherosclerosis Through Suppression of NF-κB and STAT Signaling Pathways in Diabetic Mice. *Diabetes* 64:3600-3613, 2015
5. Mallavia B, Oguiza A, Lopez-Franco O, Recio C, Ortiz-Munoz G, Lazaro I, Lopez-Parra V, Egado J, Gomez-Guerrero C: Gene Deficiency in Activating Fcγ Receptors Influences the Macrophage Phenotypic Balance and Reduces Atherosclerosis in Mice. *PLoS One* 8:e66754, 2013
6. Recio C, Oguiza A, Mallavia B, Lazaro I, Ortiz-Munoz G, Lopez-Franco O, Egado J, Gomez-Guerrero C: Gene delivery of suppressors of cytokine signaling (SOCS) inhibits inflammation and atherosclerosis development in mice. *Basic Res Cardiol* 110:8, 2015

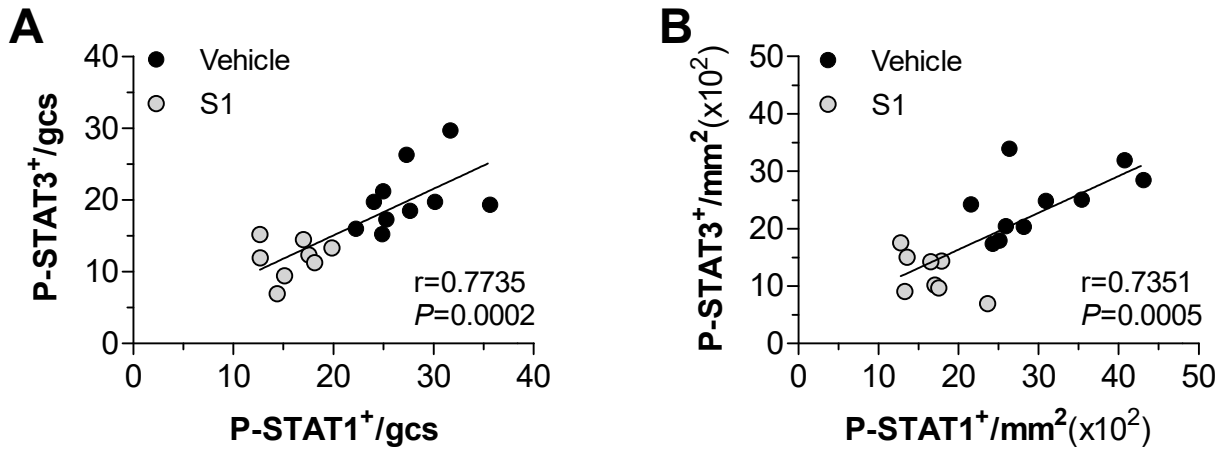
7. Ortiz-Munoz G, Lopez-Parra V, Lopez-Franco O, Fernandez-Vizarra P, Mallavia B, Flores C, Sanz A, Blanco J, Mezzano S, Ortiz A, Egido J, Gomez-Guerrero C: Suppressors of cytokine signaling abrogate diabetic nephropathy. *J Am Soc Nephrol* 21:763-772, 2010
8. Mallavia B, Recio C, Oguiza A, Ortiz-Munoz G, Lazaro I, Lopez-Parra V, Lopez-Franco O, Schindler S, Depping R, Egido J, Gomez-Guerrero C: Peptide inhibitor of NF-kappaB translocation ameliorates experimental atherosclerosis. *Am J Pathol* 182:1910-1921, 2013

Supplemental Figure S1 (Recio et al.)



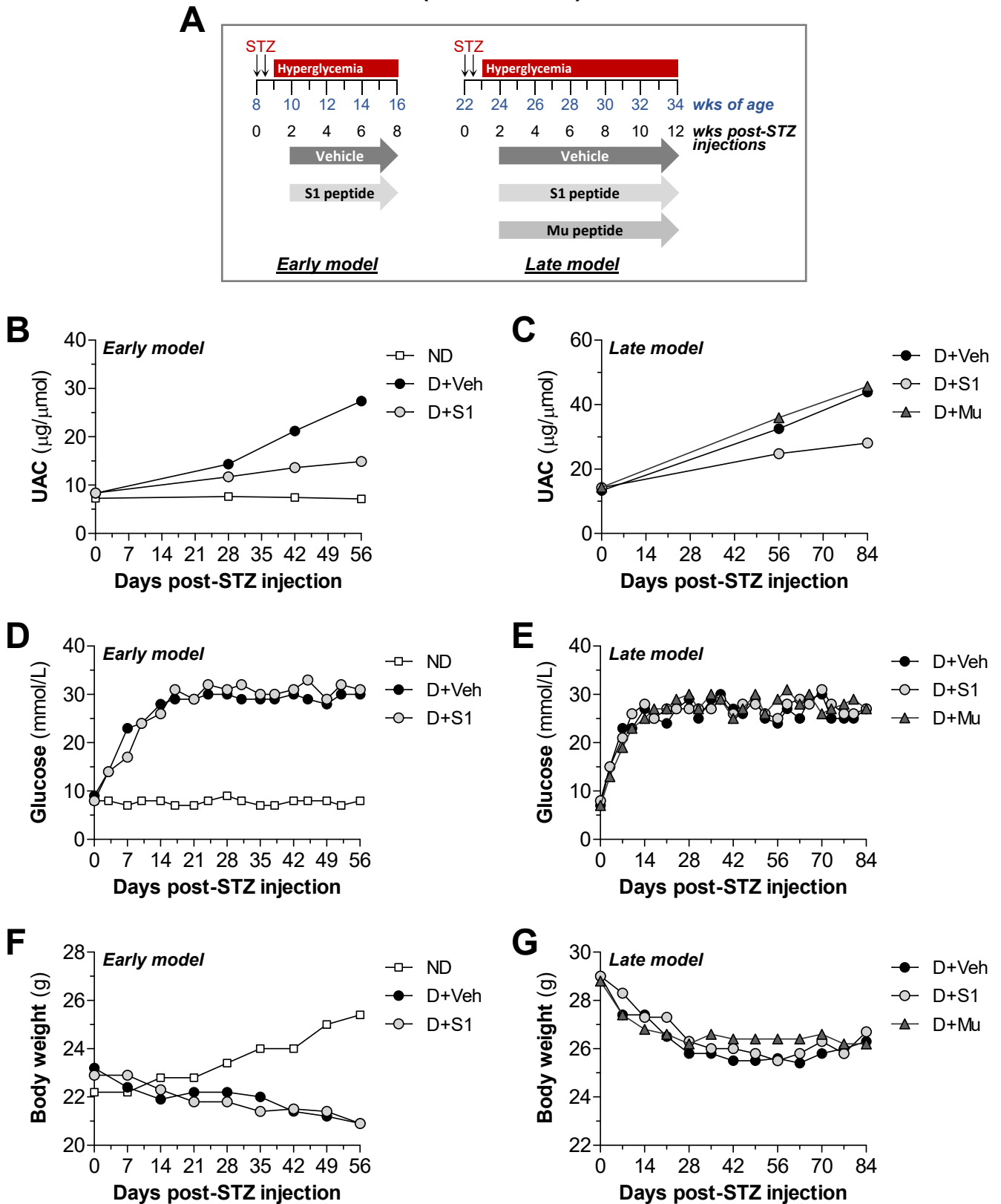
Biodistribution and pharmacokinetics of SOCS1 mimetic peptide in ApoE-deficient mice. (A) *Ex vivo* fluorescence microscopy images of mouse tissue sections at 6 h of intraperitoneal injection of either vehicle or rhodamine-labeled SOCS1 peptide (magnification x200; red, S1; blue, DAPI labeled nuclei). Dotted lines indicate glomerular area; asterisks indicate tubular cells. (B) Quantification of red fluorescence in tissue samples over time (n=4) was expressed as relative fluorescence per g of tissue. (C) Fluorescence in plasma and urine at different time points (n=2-3 per time point). (D) Plasma fluorescence data were normalized, plotted in a logarithmic scale versus time post-injection, and fitted by nonlinear regression to a one-phase exponential decay function ($R^2=0.976$).

Supplemental Figure S2
(Recio et al.)



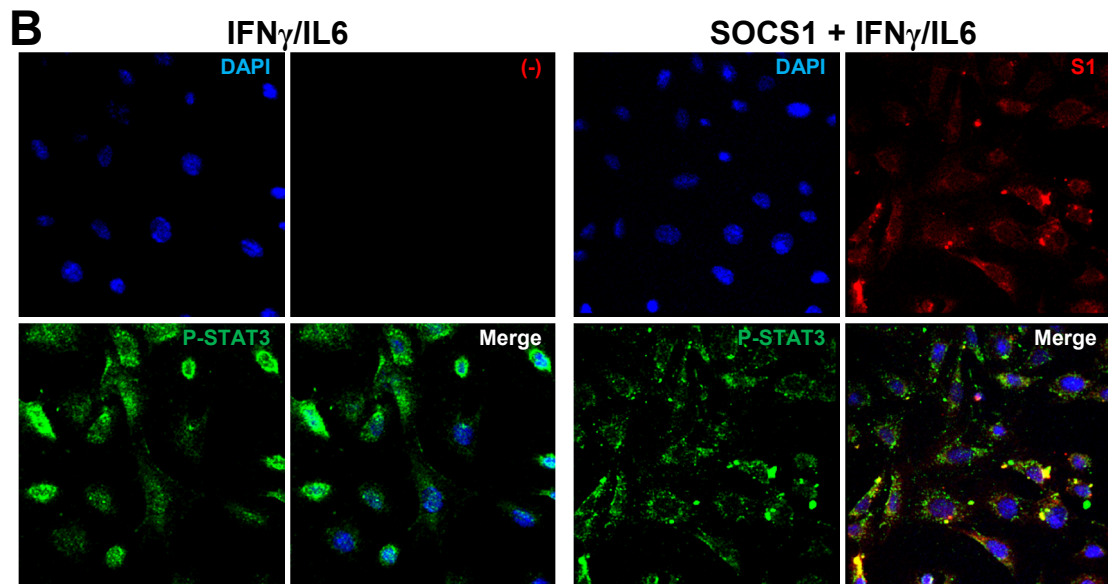
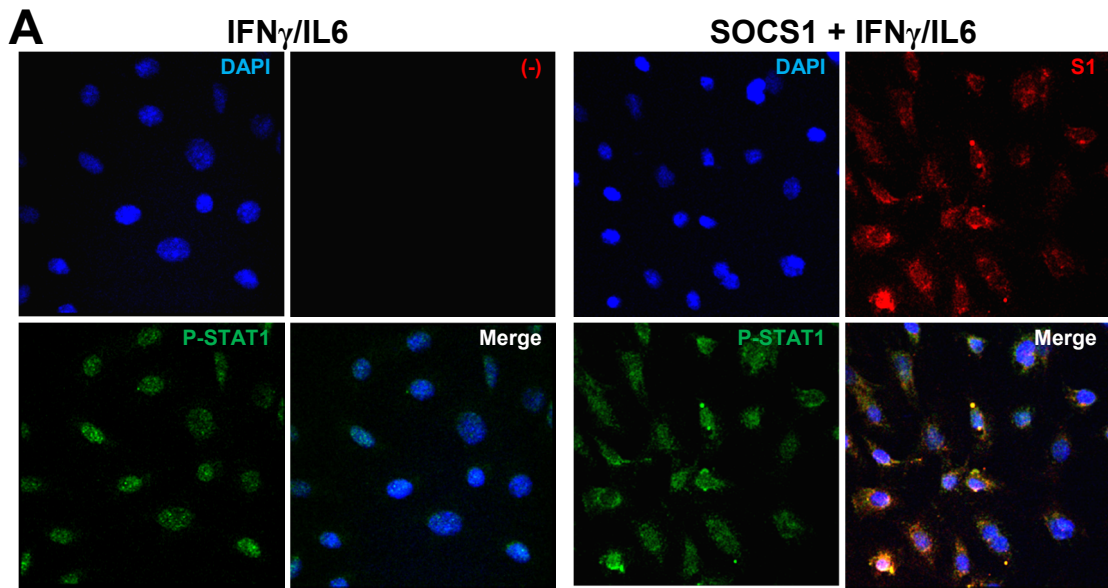
Correlation of STAT activation levels in diabetic mice. Pearson's correlation analysis of STAT1 versus STAT3 activation in glomerular (A) and tubulointerstitial (B) compartments.

Supplemental Figure S3 (Recio et al.)

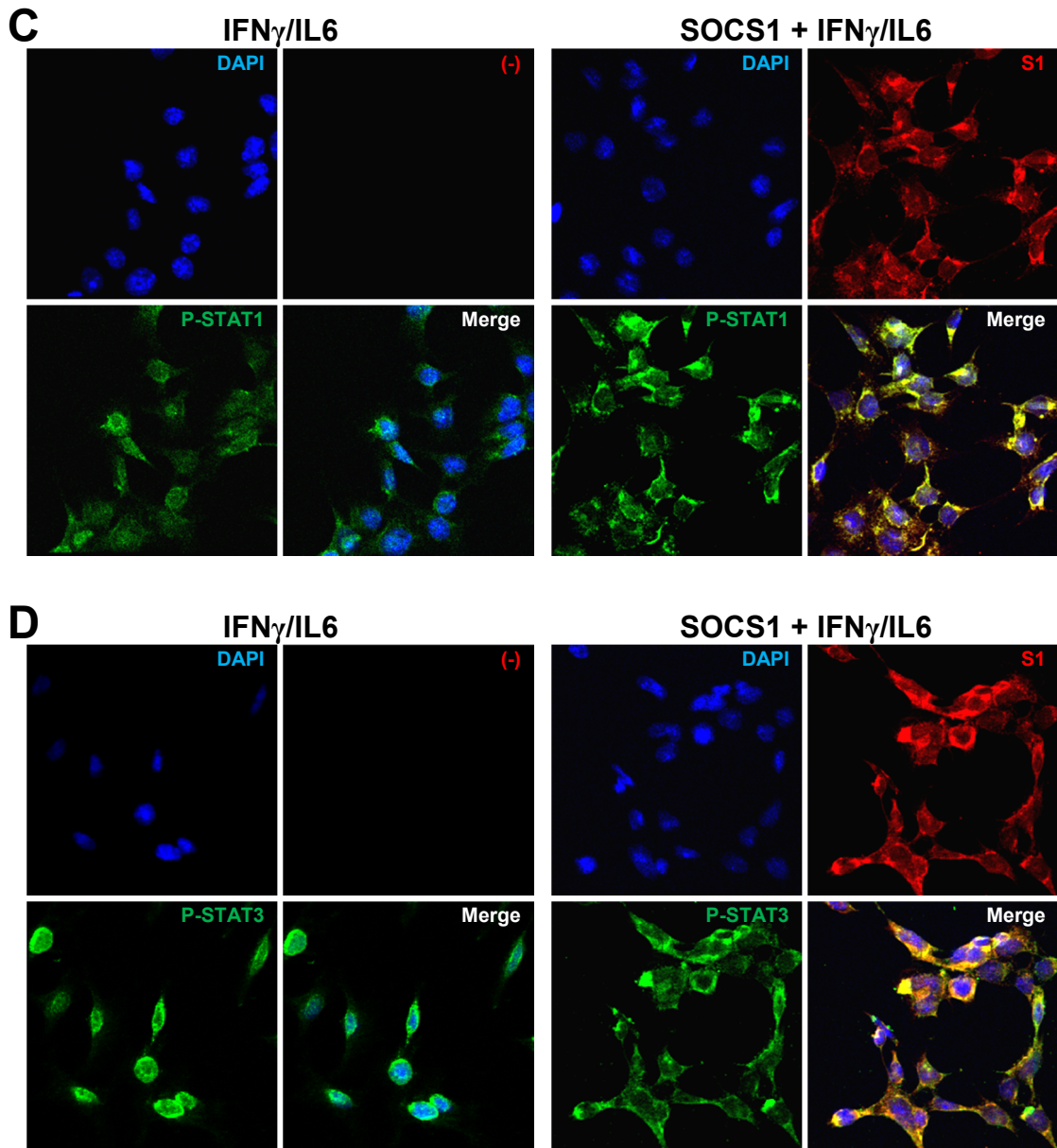


Experimental model of diabetes in ApoE-deficient mice and treatments. (A) Scheme of experimental procedure. (B-G) Evolution of urine albumin-to-creatinine ratios (B, C), blood glucose levels (D, E) and body weights (F, G) in the experimental groups of mice at early and late treatments. Average values of 3-10 animals per group are represented. ND, non-diabetic; D, diabetic; Veh, vehicle; S1, SOCS1 peptide; Mu, mutant peptide.

Supplemental Figure S4
(Recio et al.)

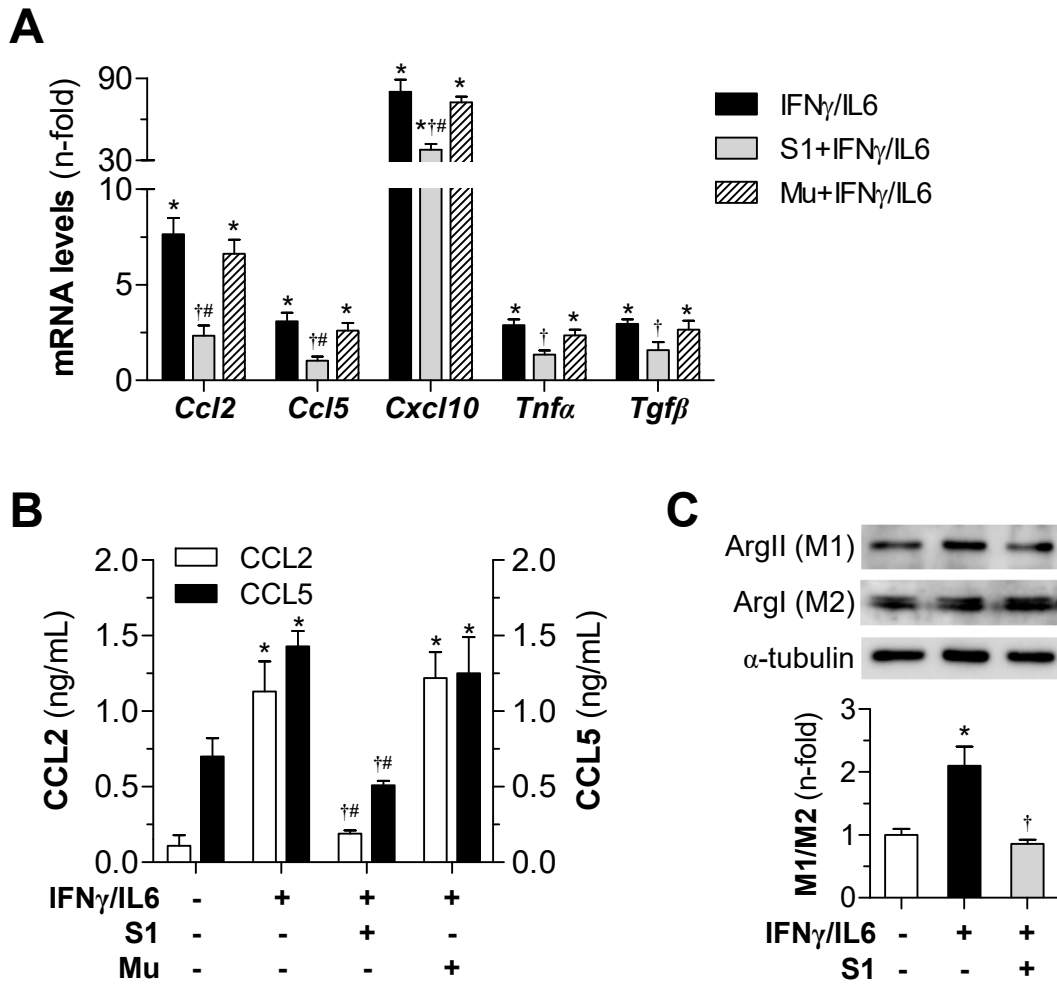


**Supplemental Figure S4
(Recio et al.)**



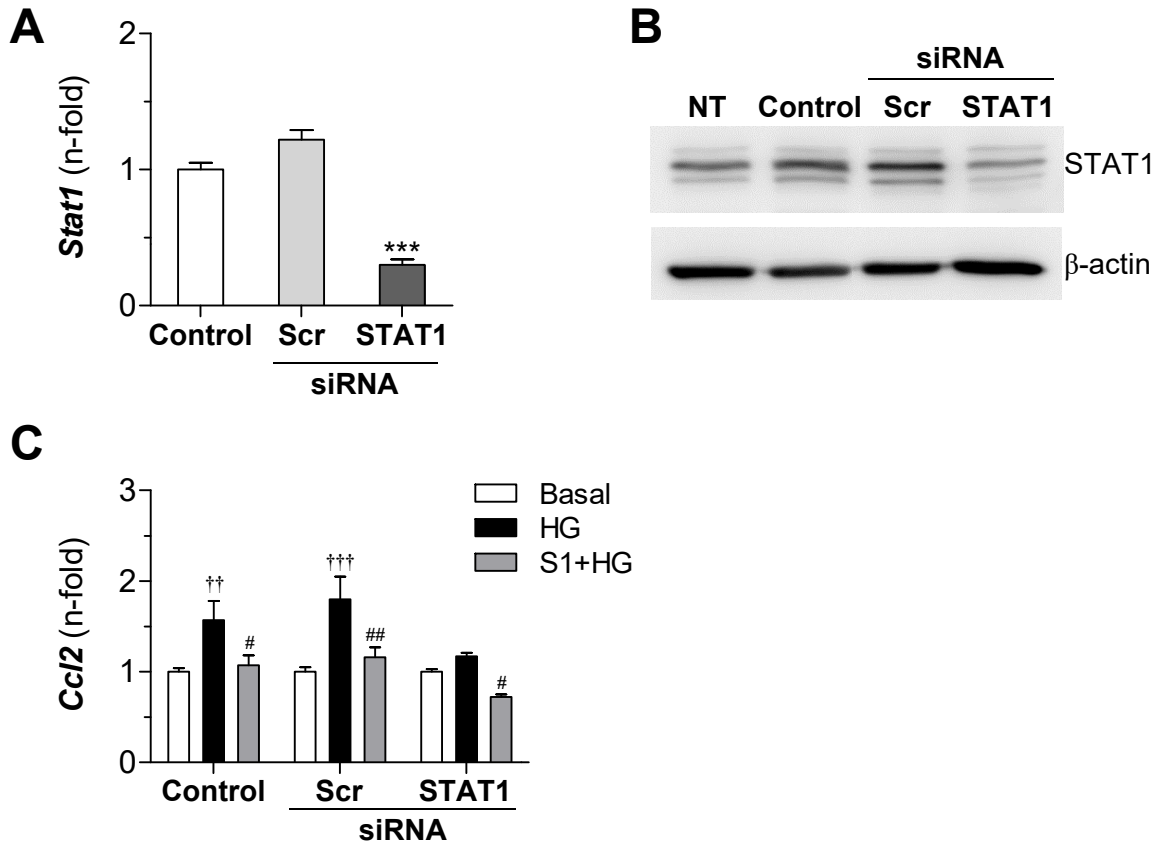
SOCS1-derived peptide inhibits STAT activation in cultured renal cells. Cultured mesangial cells (MC) (**A, B**) and tubuloepithelial cells (MCT) (**C, D**) were stimulated with cytokines (10^3 U/mL IFN γ plus 10^2 U/mL IL-6; 60 min) in the absence or presence of rhodamine-labeled peptide (S1, 100 μ g/mL). Cells were then fixed and stained for P-STAT1 (**A, C**) and P-STAT3 (**B, D**). Representative confocal fluorescence images of four separate experiments (red, S1; green, P-STAT1/P-STAT3; blue, DAPI stained nuclei).

Supplemental Figure S5 (Recio et al.)



SOCS1 peptide inhibits cytokine mediated responses *in vitro*. Quiescent cells were preincubated with SOCS1 peptide sequences (S1 and Mu; 100 μ g/mL, 90 min) before cytokine stimulation (10^3 U/mL IFN γ plus 10^2 U/mL IL-6). **(A)** Real-time PCR analysis of indicated genes in MC at 24 h of stimulation. Values normalized by 18S are expressed as fold increases over basal conditions (arbitrarily set to 1). **(B)** CCL2 and CCL5 concentrations in supernatants from cytokine-stimulated MCT measured by ELISA. **(C)** Protein expression of arginase isoforms (ArgII and ArgI) in mouse macrophages. Representative immunoblots and summary of the relative levels of M1 (ArgII) and M2 (ArgI) markers are shown. Bars represent the mean \pm SEM of duplicate determinations from 4-6 independent experiments. *P<0.05 versus Basal, †P<0.05 versus Cytokines, #P<0.05 versus Mu.

**Supplemental Figure S6
(Recio et al.)**



STAT1 silencing and SOCS1 peptide similarly inhibit CCL2 expression *in vitro*.

MCT were transfected with vehicle (Control), scramble siRNA (Scr) and specific siRNA for STAT1 (30 nmol/L, 24 h). **(A)** Gene expression levels of STAT1 in unstimulated MCT. RT-PCR data normalized by 18S are expressed as fold increases versus Control. **(B)** Representative immunoblot of STAT1 protein expression (n=3) in non-transfected (NT) and transfected cells. **(C)** Real-time PCR analysis of CCL2 in MCT at 16 h of stimulation with high-glucose (HG, 30 mmol/L D-glucose) in the presence or absence of SOCS1 peptide (100 μ g/mL, 90 min pretreatment). Bars represent the mean \pm SEM of duplicate determinations from 3-5 independent experiments. ***P<0.001 versus Control transfection; †P<0.05, †† P<0.01 versus Basal; #P<0.05, ## P<0.01 versus HG.